

# Modelling heat recovery from urban wastewater systems

- Case study from Malmö



Diego Reyes

---

Water and Environmental Engineering  
Department of Chemical Engineering  
Master Thesis 2019



MODELING HEAT RECOVERY FROM  
URBAN WASTEWATER SYSTEMS  
- CASE STUDY FROM MALMÖ

by

Diego Reyes

Master Thesis number: 2019-2

Water and Environmental Engineering  
Department of Chemical Engineering  
Department of Industrial Electrical Engineering and Automation  
Lund University

May 2019

Supervisor: **Dr. Ramesh Saagi, IEA, Lund University**

Co-supervisor: **Dr. Magnus Arnell, RISE**

Examiner: **Senior Lecturer Åsa Davidsson, Lund University**



# Preface

Being sustainable, that is the goal for every human being on this planet. Reusing resources to reduce consumption patterns is one key to reaching this goal. For that reason, after several years of studying the relationship between human activities and the corresponding effects of those activities on the planet earth, I was fascinated by the opportunity to work on a topic that would allow me to significantly contribute to a field hungry for research: recovery of energy traditionally wasted in wastewater treatment processes. Thus, the focus of this project, modeling heat recovery from wastewater systems, focuses on the goal of sustainability by showing how cities can mitigate some of the impact of an essential human activity through leveraging the potential of the already built sewer systems.

This thesis has been written to fulfill the graduation requirements of the master's degree in Water Resources Engineering at Lund University. I was engaged in researching and writing this study from January to May 2019. This was a remarkable journey due to the combination of field and office work that allowed me to understand different points of view on the connections between the different topics analyzed.

I would like to thank my supervisor, Dr. Ramesh Saagi, for his outstanding and admirable guidance and support during this process. I also want to thank all the people involved in the project: Irmeli Grongstad, from the Environmental Lab at VA Syd; Christoffer Wärrff, project manager at RISE; Ulf Jeppsson, associate professor and deputy head of department at Lund University; and Magnus Arnell, project manager at RISE. Equally as important, I need to give a big thank you to my parents, especially my mom, who has always been here to support and motivate me. Her example and advice showed me the most beautiful path to follow.

Finally, I wish to thank my readers and express my sincere wish that, in reading this paper, you will be inspired to reflect on the debt we each owe to this miraculous planet and will be encouraged to implement solutions to reach sustainable ways of living.

Diego Reyes González

Lund, Sweden, June 2019



# Summary

The purpose of this thesis is to estimate how much heat can be recovered from the sewer system in Malmö, Sweden, and determine the best location for that heat recovery. In fulfilling that purpose, this thesis covers the process of modeling wastewater flows and temperature changes in the sewer system in Malmö, the results of those processes, and the estimated amount of heat that can be recovered from the sewer system. The methods used to complete this study included primary data collection through in-sewer equipment installation and field data measurements, along with the use of two different models (one for a city-wide wastewater flow rate prediction and the other regarding heat transfer in the sewer network). Extensive secondary research was also conducted. The results from this study included the estimation of different amounts of heat from the sewer system. For example, a scheme of heat extraction of 36,000 kW during a 12-hour period was analyzed during the same time frame where flow and temperature data was collected. That number would always keep a temperature at the wastewater treatment plant over 9 °C and corresponds to 6.3% of the total district heating consumption per year in Malmö. Also, a 1% difference between the real and modeled wastewater flows for one of the catchments on the city was obtained. Finally, the temperature modeling process delivered differences between 0.1 and 0.3 °C for one of the studied places.





# Table of Contents

<b>1</b>	<b><i>Introduction</i></b> .....	<b>1</b>
1.1	Overview .....	1
1.2	Aim.....	2
1.3	Objectives.....	2
1.4	Roadmap.....	2
<b>2</b>	<b><i>Literature Review</i></b> .....	<b>3</b>
<b>3</b>	<b><i>Materials and Methods</i></b> .....	<b>5</b>
3.1	The process of modeling the flow rate dynamics in the sewer system at a city-wide scale in Malmö .	5
3.1.1	Modeling of the Catchment and Sewer Network sub-models .....	5
3.1.2	Data of the place under study .....	6
3.2	Process of modeling the temperature dynamics in the sewer system at a city-wide scale in Malmö .	12
3.2.1	Modeling temperature variations in the sewer system.....	12
3.2.2	Modeling heat recovery from the sewer system .....	14
3.2.3	Characteristics and data measurements from the stretches under study .....	14
<b>4</b>	<b><i>Results and Discussion</i></b> .....	<b>19</b>
4.1	Modeling the flow rate dynamics in the sewer system at a city-wide scale in Malmö.....	19
4.1.1	Modeling the Catchment and Sewer Network sub-models.....	19
4.2	Modeling the temperatures dynamics in the sewer system at a city-wide scale in Malmö...	23
4.2.1	Analysis of field data .....	23
4.2.2	Modeling temperature variations in the sewer system.....	27
4.2.3	Modeling heat recovery from the sewer system .....	31
<b>5</b>	<b><i>Conclusions</i></b> .....	<b>37</b>
<b>6</b>	<b><i>Future Work</i></b> .....	<b>39</b>
<b>7</b>	<b><i>References</i></b> .....	<b>41</b>
	<b><i>Table of Abbreviations</i></b> .....	<b>45</b>
	<b><i>Appendices</i></b> .....	<b>47</b>



# 1 Introduction

## 1.1 Overview

Water is an essential need for human development and is a vital resource for life on the planet earth. Since it is wrongly categorized as a renewable resource, it is taken for granted and is often used without limitation. According to the United Nations Educational, Scientific and Cultural Organization (UNESCO), water usage has been estimated at about 4,600 km<sup>3</sup> per year and is projected to increase to around 6,000 km<sup>3</sup> by 2050 (UNESCO, 2018). Additionally, in 2018, 844 million people were living without access to safe water and 2.3 billion were living without access to improved sanitation (Water.org, 2018).

In addition to water being overused, water is often made unsafe due to human activity. Contamination of water resources around the world can be partially attributed to urbanization, as is often reflected in the ecosystems around urban areas. An all-to-common example of the impact of urban areas are the extreme cases of irreparable damage to nearby ecosystems caused by the eutrophication that results from the discharge of municipal wastewater into natural receiving waters (Grmela *et al.*, 2014). Simply put, at our current rates of consumption and waste generation, we are moving towards a time when access to fresh water will be greatly diminished for a growing percentage of the population. This is not to say that we are without hope. If water was to be considered as a limited resource, and sustainable techniques for its use were to be paired with conservation efforts in the most demanding and damaging areas, such as urbanized places, then the potential negative effects brought on by a lack of access to fresh water may be mitigated.

Along with household uses of water, the energy input required for the urban water cycle also impacts water's availability in many ways. For example, water is used as a source of energy in hydropower generation, and it is used to create other types of energy such as thermoelectric and that from oil and coal exploration. Olsson (2012) explains the relationship between these two elements – the energy needed to extract, treat, and transport water, and the water needed to create energy by different means – highlighting how there is an interdependency between them. In other words, in the traditional urban model, the more energy needed to extract, treat, and transport water, the more water we use to produce that energy. Thus, for sustainability purposes, the need to develop and implement tools that diminish the consumption of energy in the urban water cycle is self-evident.

Tools that reduce the use of energy in the urban water cycle can likely have the greatest impact if they address the most energy demanding activity in the whole urban water system: household water heating. This activity requires massive amounts of energy compared with the rest of the water-related activities in the urban water cycle, even more than the treatment of wastewater (Olsson, 2012). One reason household water heating requires so much energy is that each unit of energy often provides little utility. Water in households is usually heated and used for a few seconds, then is immediately wasted through the sinks and transported via underground pipes in the sewer transit network to the wastewater treatment plant. In some wastewater treatment systems, energy is obtained by the biological reactions that break down the waste through the anaerobic decomposition of organic material creating methane (biogas). However, after treatment, the reuse of wastewater as a source of heat energy generation is often unexploited due to the lack of awareness and proper technology (Mikkonen *et al.*, 2013). Thus, there is still a need for other tools to recover the heat energy wasted through household water use.

One such tool to recover wasted heat energy is heat recovery. Like biogas-capture, this solution also has the potential to reduce the net consumption of energy in the urban water system as a whole. Because a reduction in the net consumption of energy in the urban water system correlates to a reduction in the use of freshwater resources, the implementation of heat recovery technology presents a solution for one of the fundamental problems facing the sustainable development of urban areas.

## **1.2 Aim**

In addition to supporting the development of heat recovery technology, this project aims to address two key aspects related to the development of sustainable infrastructure: First, the importance of modeling on a city-wide scale and how such modeling can facilitate the decision-making process and lower costs of heat-recovery projects overall. And, second, emphasizing the importance of finding ways to be sustainable in all aspects of human development, including those activities that consume an overwhelming amount of resources. Additionally, the results from this thesis will become a foundational part of the new knowledge base that is being created around the amazing topic of heat recovery; a topic that, for the reasons outlined above, will be likely crucial for the sustainable development of cities in the future. Also, in reaching these findings, this thesis attempts to demonstrate how simplified models can be used to describe flow rate and temperature changes in the sewer system.

## **1.3 Objectives**

Prior to the adoption of heat recovery systems, one fundamental question that must be answered is how much heat can be captured during transit without negatively impacting the efficiency of the biological processes at the wastewater treatment plant. Therefore, the research questions involved in this thesis project include:

1. Can flow rate dynamics be described for the sewer system in Malmö using a conceptual flow model?
2. Can the temperature variation in a sewer system be predicted using detailed one-dimensional heat transfer model?
3. What are the effects of recovering heat from wastewater in the sewer network on the influent temperature at the wastewater treatment plant?
4. Can a heat transfer model for the sewer system be linked with a city-wide flows model?
5. What is the most suitable alternative for heat recovery from the sewer system in Malmö?

## **1.4 Roadmap**

To answer the research questions, the below steps were followed:

1. Installation of equipment and the collection of the necessary data for the description of the whole system and to use it as an input for the modeling process.
2. Modeling of the wastewater flow rate in the sewer system using a flows model for the three catchments in Malmö that convey the water to the wastewater treatment plant.
3. Modeling the temperature changes in the sewer network using a heat transfer model.
4. Estimating different amounts of heat that can be recovered in different scenarios, developing a connection between the flows and temperature models, and estimating the most suitable alternative for heat recovery from the sewer system in the city.

## 2 Literature Review

Wastewater is already used as a component of heating and cooling processes in buildings via heat pump technology. The implementation of this technology started more than 20 years ago and has been tested in several places around the world. For example, there are over 500 wastewater heat pumps in operation worldwide and different configurations have been implemented with successful results in Switzerland and Germany (Schmid, 2008). The sewer systems, however, are still a sink for this resource.

Prior to implementing heat extraction technology in sewage systems, the heat extraction procedures need to be studied extensively to avoid undesired effects in the systems downstream from extraction points. One example of these undesired effects is the potential negative impact of continuous heat recovery on wastewater treatment facilities. Recovering too much heat upstream of a treatment plant could lead to a lower influent wastewater temperature at the treatment plant, which will reduce the nitrification capacity and create higher effluent ammonium concentrations (Wanner *et al.*, 2005). This is one of the reasons why using computerized models that predict temperature changes in sewer systems is useful.

In 2008, it was estimated that 6,000 GWh of thermal energy are lost per year in Switzerland via the sewage system and that, between 15 to 30 percent of the input thermal energy provided to conventional buildings is lost via the sewage system. On the other hand, the same study by Schmid (2008), demonstrated how the potential efficacy of wastewater heat recovery systems is self-evident in locations where it has been successfully implemented. One such location is in Oslo, where a whole neighborhood has been provided with energy recovered from wastewater for the last 20 years by using two wastewater heat pumps that supply 80% of the energy production. Another successful project was in a house for the elderly in Switzerland, where a 30-kW heat pump has achieved an annual coefficient of performance (COP, is the ratio of the energy output to the energy input) of 3.8. For that project, it was reported that the wastewater heat pump powered with electricity from Swiss power stations produced just 22% of the CO<sub>2</sub> emissions that would have been created with an oil-fired heating system (Schmid 2008).

Similarly, Frijns *et al.* (2013), recognized wastewater as a source for energy gain through heat recovery. In their paper, they estimate a heat recovery potential of 15.6 TWh/y for domestic wastewater in the Netherlands, assuming a complete recovery and an output water temperature from the households of 27 °C. They note that the energy demand to warm up tap water in houses, about 29.4 TWh/y, was almost eight times more than that of water production and treatment, which totaled 3.8 TWh/y. Additionally, they compare the carbon footprint between the Dutch public water sector and the energy used to heat water in Dutch homes. It is estimated that the public water sector creates 1.67 million tons of CO<sub>2</sub> per year, which pales in comparison to the contribution of CO<sub>2</sub> derived from warming up tap water in households, which reaches 7.5 million tons of CO<sub>2</sub> per year. That is five times more CO<sub>2</sub> than is produced by the whole public water sector. Finally, they also recognize the need for additional research on how the changes in temperature caused by heat recovery will affect the processes downstream at the wastewater treatment plants.

Studies that have looked at modeling heat recovery strategies include those by Dürrenmatt and Wanner (2014); Abdel-Aal *et al.* (2014); and Sitzenfrey *et al.* (2017). These studies argue that heat extraction from wastewater pipes can be modeled using mathematical representations of

reality, where assumptions are needed in order to keep the models manageable and reach acceptable results from the modeling process. They also discuss that there are parameters with high sensitivity within the model and concluded important facts useful for this study. For example, Dürrenmatt and Wanner (2014) stated that successful planning and operation of heat recovery from wastewater in sewers requires analysis of the specific conditions present in any given potential application. Those conditions include the properties of the sewer system, the diurnal and seasonal variations of the wastewater discharge and temperature, legal restrictions on the downstream wastewater temperature, and the demand and available supply of energy for heating or cooling. Likewise, Sitzenfrei *et al.*, (2017) investigated different levels of implementation of decentralized systems (at the household level). They concluded that there would be an estimated maximum performance drop of 40% for a centralized energy recovery system (at the sewer network level) when all bathrooms in the study were equipped with decentralized recovery systems. Also, Abdel-Aal *et al.* (2014), explained that the cooled wastewater resulting from an upstream extraction, can potentially be reheated by the in-sewer air and ambient soil, with the goal of the wastewater reaching in-sewer air and soil temperatures. However, recovering heat at such a large scale requires long sewer pipes for the wastewater to regain the original wastewater temperature, and according to Florides and Kalogirou (2005), short-period soil temperature variations, such as daily changes between 0.25 m to 1 m deep, are small and the change cannot be observed below a depth of 1 meter. Finally, Dürrenmatt and Wanner (2014) recognized that the heat stored in the pipe walls during the day can be released into the wastewater in the early morning, as long as the temperature in the walls is higher than the water. findings provided information about how models can be implemented, and some aspects that affect the modeling process of heat recovery actions.

The debate around heat recovery also centers on the issue of how precise and detailed the models need to be in order to give an adequate approximation of the conditions that affect the changes in wastewater temperature (soil temperature, pipe thickness and material, flows magnitude, among others). Models in specific places have shown adequately estimated wastewater temperature. For example, for a measured upstream wastewater temperature of 18.8 °C, the modeling software Tempest predicted a downstream temperature of 17.9 °C, whereas the average of the measured downstream temperature was 17.5 °C (Dürrenmatt and Wanner, 2008). Similarly, Abdel-Aal *et al.* (2018), developed a network heat transfer model to assess the viability of heat energy recovery scenarios in a city-wide sewer network. In their study, the estimated heat recovery varied from 116 MWh/day in January to 207 MWh/day in May, with an assumed 100% efficient recovery and resulting wastewater temperatures above the thresholds of 5 °C in the network and 9 °C in the WWTP influent.

Describing a city-wide sewer system scenario through modeling is open, therefore, to continuous research and development that can provide more detailed analysis of the potential opportunities for and effects of heat recovery on a city-wide scale. An accurate model and resulting information would have a big impact on the decision-making process for a city like Malmö as it aims to become more sustainable. There is where the uniqueness of this thesis is: it will allow for the first steps in the simulation of the modeling of temperature in the sewer system, at a city-wide scale in Malmö, before and after the implementation of heat recovery alternatives.

## 3 Materials and Methods

### 3.1 The process of modeling the flow rate dynamics in the sewer system at a city-wide scale in Malmö

The modeling process for this part was done using a freely distributed open-source toolbox to predict the behavior of urban wastewater systems, Benchmark Simulation Model for Urban Wastewater Systems (BSM-UWS) (Saagi *et al.*, 2016). The models inside the toolbox describe the dynamics of flow rate and pollutants within the catchments, sewer network, wastewater treatment plant (WWTP), and the receiving water bodies for a hypothetical urban water system (Saagi *et al.*, 2017). The models are available for use in the MATLAB computing environment. The simulation model is comprised of four sub-models: (1) Catchment; (2) Sewer Network; (3) Wastewater Treatment Plant; and, (4) River Water System. For this project, only the Catchment and Sewer Network sub-models were used.

#### 3.1.1 Modeling of the Catchment and Sewer Network sub-models

The Catchment sub-model can simulate the dynamic profiles for wastewater generation during dry and wet weather. The generation of wastewater at each sub-catchment is achieved by combining the contributions from domestic, industry, and stormwater flows, and infiltration to sewers. For this case, the input from industries was removed due to the pure household-nature of the three analyzed catchments. Thus, the domestic generation, the stormwater contribution, and the infiltration to sewers are accounted for here.

The Sewer Network sub-model is the second component that covers three different elements: 1) a first-flush sub-sub-model, imitating the sudden increase of particulates at the beginning of precipitation events following a period of drought; 2) different types of storage tank sub-models, which account for detention basins that prevent discharge of rainwater into rivers during precipitation events; and 3) a transport sub-model that simulates the transport of the wastewater generated in the catchment to the WWTP. The only element used repetitively at various locations was the Transport sub-sub-model. The components of each sub-model are described in the following paragraphs.

#### *Domestic generation*

The contribution from domestic flows is modeled using diurnal variations to account for the effect of holidays and weekends in the average daily flow production. These variations are created by combining three user-defined data files containing normalized daily, weekly, and holiday profiles. Daily and weekly variations were based on measured values received from the pumping stations in Malmö. This accounted for the differences in the flow dynamics for the catchments and the influence of the daily changes in flows.

#### *Stormwater contribution*

The stormwater flow rate was calculated considering the impervious areas and rainfall runoff coefficients for each catchment to determine the amount of runoff to the sewer system. The rainfall on the permeable areas, on the other hand, was assumed to reach the groundwater and serves as an input for the other modules of the model, namely, those that comprise the infiltration to the sewers. Additionally, in this part, the input precipitation was converted from the precipitation intensity, in mm/h, into surface runoff, in m<sup>3</sup>/d. This was done using a dimensionless rainfall runoff coefficient, the impervious area, and the factors for the conversion of

units. Precipitation data obtained from the Swedish Meteorological and Hydrological Institute (SMHI) was processed in this part as well.

**Infiltration to sewers**

The contribution of the infiltration to the sewers included a groundwater conceptual block. That block described changes in the amount of infiltration attributed to variations in the groundwater level over the year and was modeled as a sine wave with a yearly frequency. Its lowest values were present during the dry period and the highest during the rainy period. The other element that influenced the infiltration to sewers was a soil conceptual block with a variable volume tank to model the percolation of surface runoff to the soil during precipitation events. The output from the tank is the infiltration to the sewer system determined by a non-linear relationship between the tank level and the infiltration flow rate. For this case, the flows resulting from that soil conceptual block needed to be ignored because it was increasing the outflow from the total infiltration contribution to the total flows.

**Transport**

This part of the model simulates the sewer system used for the conveyance of wastewater. It is formulated as a series of linear reservoirs connecting all the flows inside every sub-catchment. The number of such reservoirs is determined by the catchment area and the sewer flow that has to be conveyed through the network. For this project, a few reservoirs were added or deleted to match the actual measured flows and to avoid the lags found at every sub-catchment.

Saagi *et al.* (2016), presented a detailed explanation and examination of the Catchment and Sewer network sub-models. The mathematical expressions for the different interactions can be examined in detail in their paper. Figure 3.1. shows the visual representation of the model.

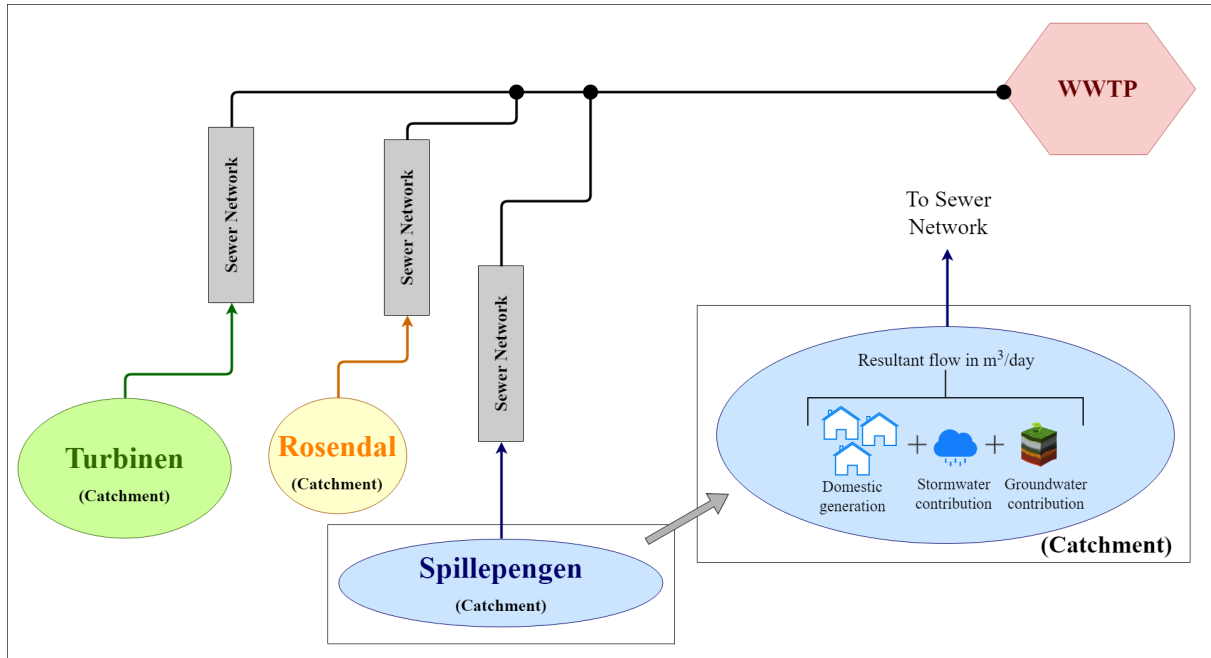


Figure 3.1. Visual representation of the BSM-UWS model with different contributions.

**3.1.2 Data of the place under study**

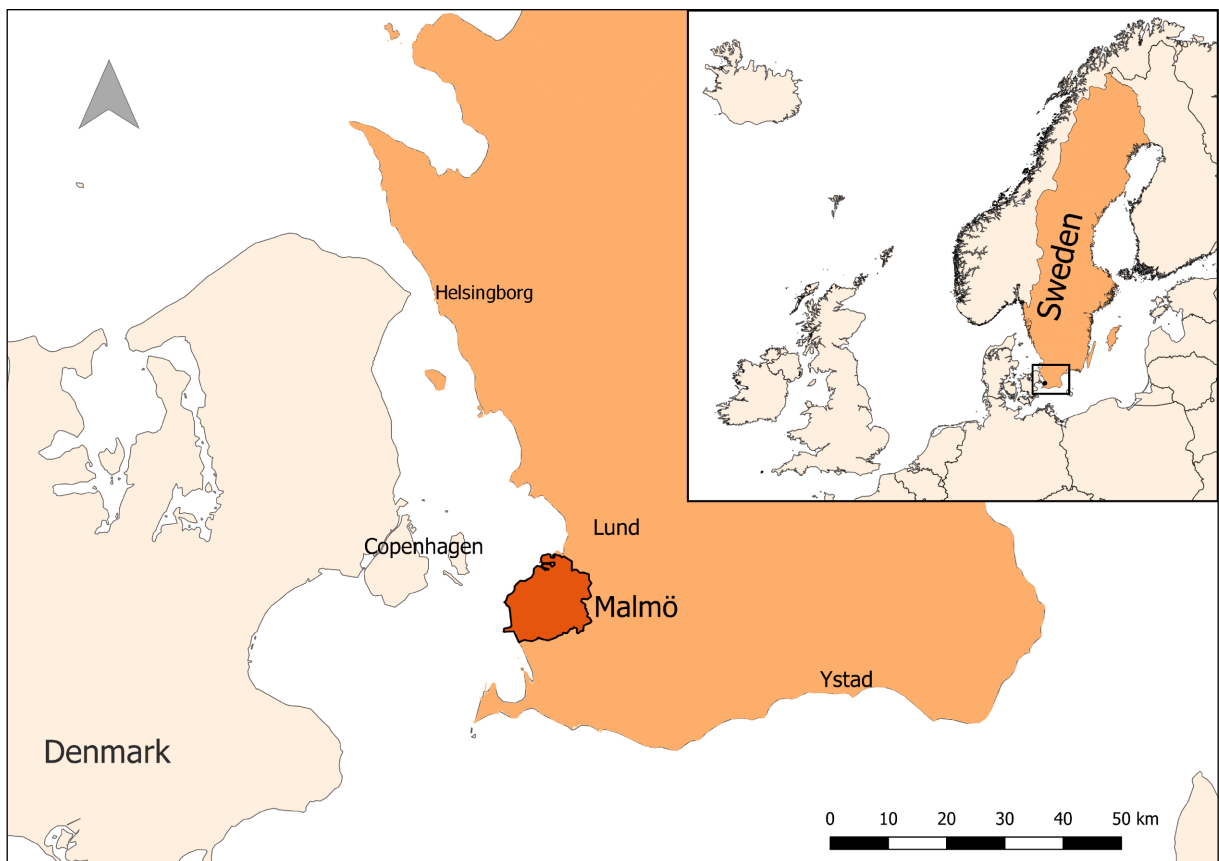
The data necessary for this study was obtained from the local water utility VA Syd, and from field tests conducted by the thesis team in collaboration with VA Syd. The data received from the water utility included historical precipitation information, GIS data, and flow measurements



for three of the main pump stations in their sewer network. Additionally, the information necessary for this study was obtained by conducting secondary research using existing data from different sources.

### **General information**

Malmö is the third biggest city in Sweden. It has a population of 333,633 (Statistics Sweden., 2018), an area of 157 km<sup>2</sup> (15,600 ha) and, as Sweden's fastest-growing city (with a 43% population growth since 1990 (which is faster than for Stockholm) (Malmö stad, 2018)), it plays an important role in the south of the country due to its commercial and industrial activity. The total energy consumption of the Malmö municipality has been around 7 TWh/year for the last 15 years. The consumption per capita for this same timeframe was around 25 MWh/year, which is lower than average for the province of Scania (33 MWh/year) and lower than the overall Swedish average (46 MWh/year). Additionally, the district heating system in Malmö requires an average of 2.5 TWh/year (33% of the city's total energy consumption) and covers over 90% of the households in the municipality (Andrén, 2009). Figure 3.2. shows the location of Malmö within Sweden.



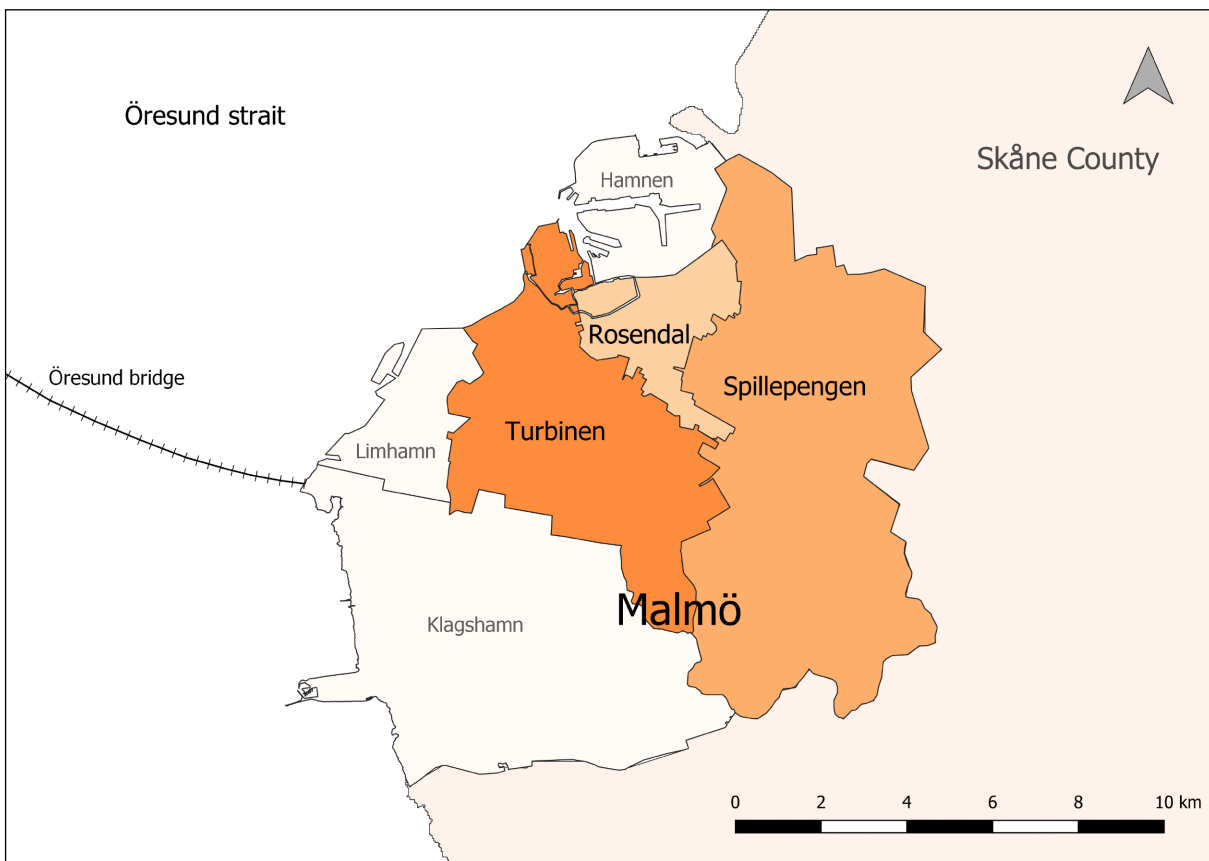
*Figure 3.2. The area under study inside the square, south of Sweden, and a zoomed view including other municipalities nearby.*

### **Catchments and sewer system**

In Sweden, the drainage systems in urban areas were designed for rainfalls of a 10-year recurrence interval (Haghighatafshar *et al.*, 2018), which are events that have a 10% probability of being equaled or exceeded in any one year. This corresponds to a rainfall volume of 16 mm in 15 min, 26 mm in one hour, and 30 mm in two hours in Malmö (Sörensen and Mobini, 2017).

The city also has a characteristic flat topography; therefore, pumping is necessary in the sewer system in order to convey the wastewater to the treatment plant.

Because this study focuses on urban areas, only the urbanized parts of Malmö were considered. This corresponds to the three catchments Turbinen, Spillepengen, and Rosendal, which transport the wastewater from the city to Sjölanda, one of the two wastewater treatment plants of the municipality. Two catchments inside the city (Klagshamn and Limhamn) are not considered because they are not connected to Sjölanda and one other is excluded because it is fully industrial (Hamnen). Figure 3.3. shows the location of the studied catchments.



*Figure 3.3. Catchments belonging to the sewer network in Malmö. This document focuses on Turbinen, Spillepengen, and Rosendal which are the ones connected to Sjölanda.*

In Malmö, there are three main pumping stations, Turbinen PS, Rosendal PS, and Spillepengen PS, located in the catchments under study. All of them are controlled automatically and are equipped with level sensors and alarms. Each pumping station has at least one spare pump that is used when needed. For example, at Turbinen and Rosendal PSs, when the inflow exceeds the maximum pumping capacity, the combined wastewater is sent with the use of the spare pump to the receiving water system in order to avoid flooding. Table 3.1 shows the areas of each catchment in hectares and their respective types of systems. Figure 3.4. shows the types of sewer systems for the pipe network of the city.

Table 3.1. Areas of each catchment and their types of systems. (Modified from VA Syd, 2017)

Catchment	Combined System		Semi-separate System		Separate System		Total Systems
	[hectares]	%	[hectares]	%	[hectares]	%	
<b>Turbinen</b>	660	34%	308	16%	975	50%	1,943
<b>Rosendal</b>	495	85%	58	10%	28	5%	581
<b>Spillepengen</b>	246	11%	44	2%	1908	87%	2,198
<b>Total</b>	1,401	<b>29%</b>	410	<b>9%</b>	2,911	<b>62%</b>	<b>4,722</b>

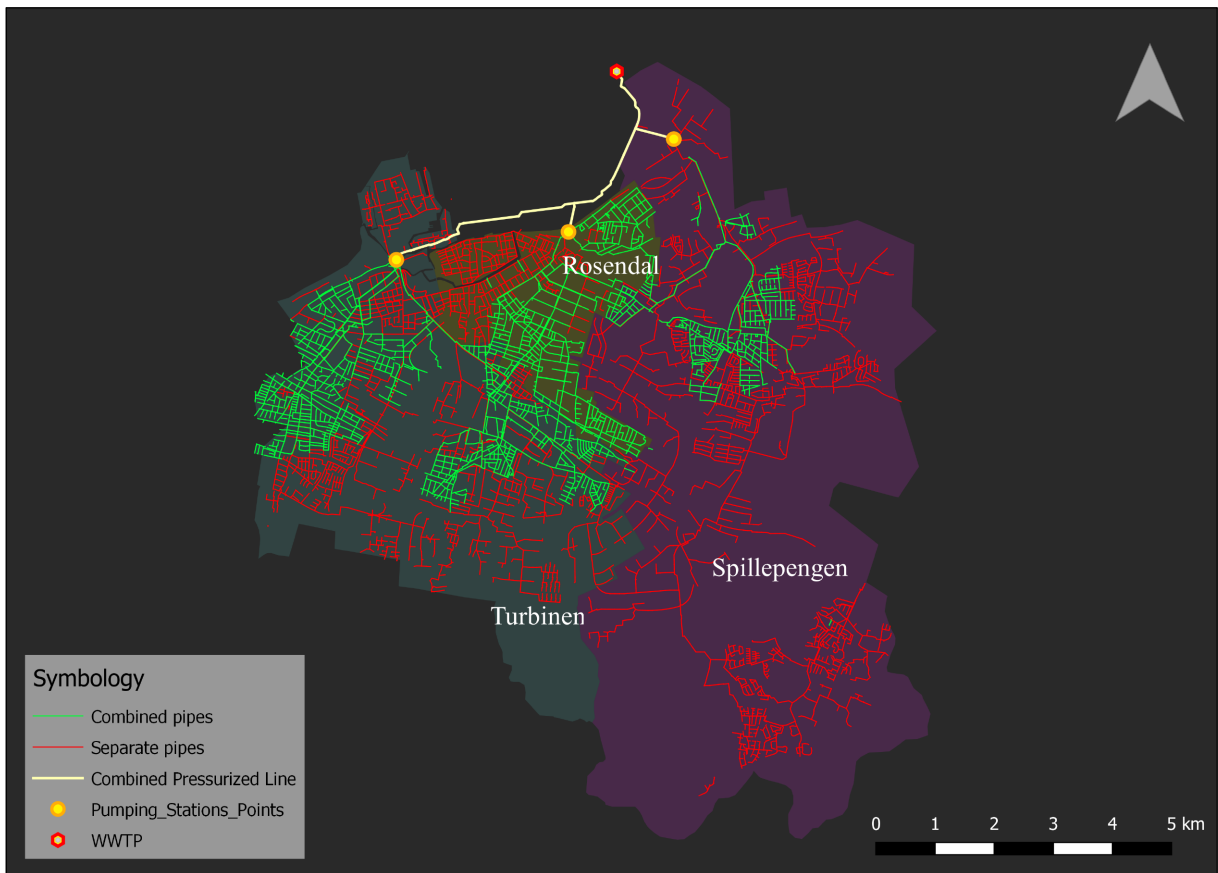


Figure 3.4. Types of sewer systems in the pipe network in the city. The protanomaly, deuteronomaly, and tritanomaly safe version can be found in Figure 0.5.

In total, in Malmö, in the three catchments analyzed in this study, 29% of the urban area has combined system, 9% has a semi-separate system, and 62% has a separate system. In the semi-separate system, the stormwater pipes are connected to a combined system downstream, whereas in the separate system, the storm and wastewater flows are conveyed in different pipes. In the total sum of areas by type of system, the absolute area of the combined and semi-separate systems is bigger in Turbinen than in Rosendal and Spillepengen. However, the same ratio (of the combined plus semi-separate systems) is bigger for Rosendal than for the other two catchments (if the analysis is done by comparing the percentages of every catchment separately). For that reason, rainfall events more significantly influence the pumping station in Rosendal. Figure 3.5 shows that distribution of percentages per system for every catchment.

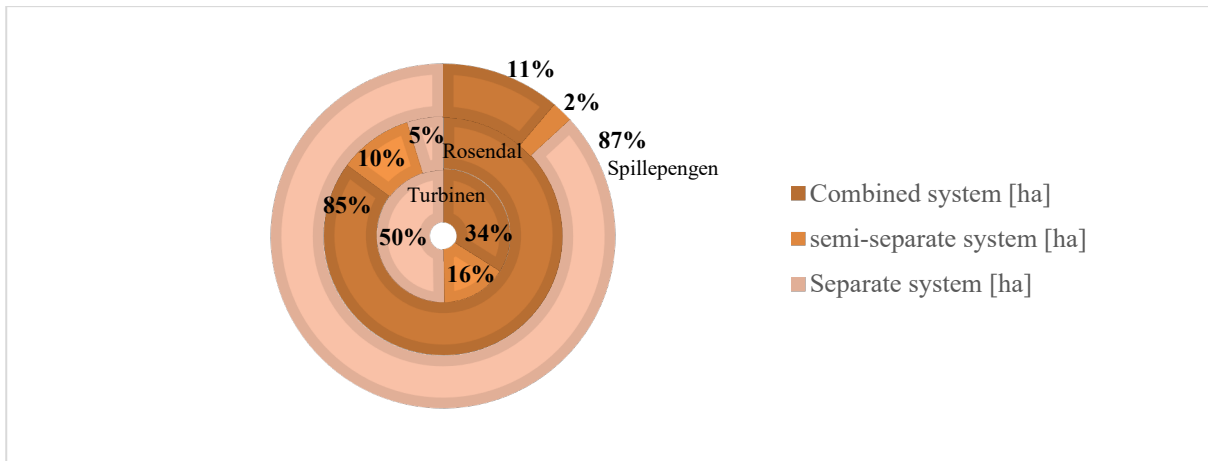


Figure 3.5. Portions of the type of sewer system in each of the catchments under study.

Additionally, the pump capacities of each station are as follows: Turbinen, 2.5 m<sup>3</sup>/s; Rosendal, 2.7 m<sup>3</sup>/s; and Spillepengen, 1.6 m<sup>3</sup>/s. All three pumping stations are connected to Sjölund, with a total maximum pressurized capacity of 8 m<sup>3</sup>/s (VA Syd, 2017). The sewer system in Malmö also has detention basins that work as surface or underground storage facilities. The detention basins provide flow control through attenuation of stormwater runoff. The total volume of the basins is approximately 52,000 m<sup>3</sup>, where 9,500 m<sup>3</sup> are for the combined system, 13,500 m<sup>3</sup> are open basins, and 29,000 m<sup>3</sup> are built as underground basins in the separate system (Sörensen and Mobini, 2017). Figure 3.6. shows the connection of the pumping stations with Sjölund.

Infiltration in the sewer system also plays an important role in the overall sum of flows in the city. Defined as all the water that is not wastewater in wastewater-conducting pipes (VA Syd, 2017), infiltration creates capacity problems such as overflows to the recipient water bodies, basement flooding, and increased internal overflow, as well as leads to the consumption of precipitation chemicals, additional energy consumption, reduced purification, and the addition of heavy metals in the sludge at the treatment plant. For example, according to the 2017 Sjölund Environmental Report (VA Syd, 2017) for the total annual inflow in Sjölund from Malmö (36 Mm<sup>3</sup> for 2017), the amount of infiltration water totaled approximately 11 Mm<sup>3</sup> from that year. That corresponds to 30.5% of the total inflow to the plant from Malmö (not including the other inputs to the WWTP excluded due to the focus of this thesis).

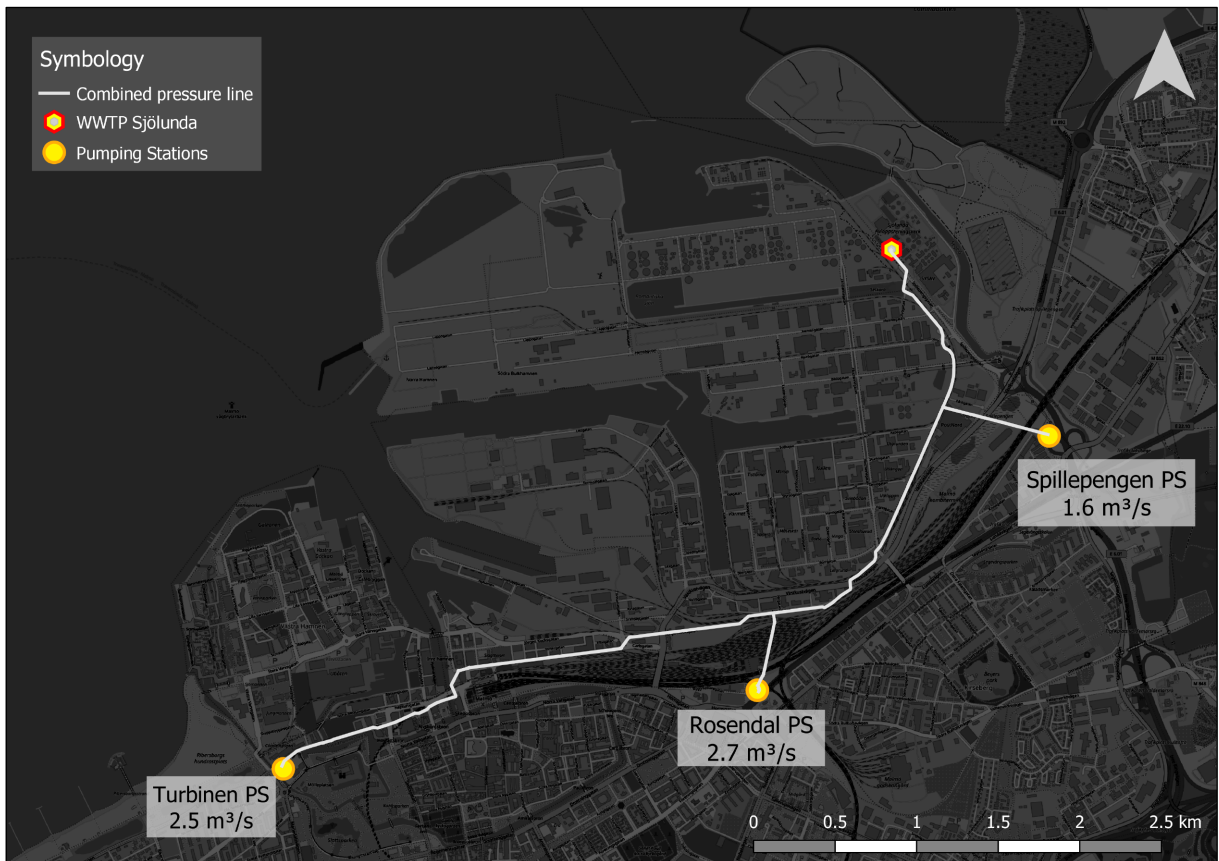


Figure 3.6. Location and capacity of the three pumping stations that transfer the wastewater to Sjölunda (based on VA Syd, 2017b, using GIS and © OpenStreetMap contributors data).

On the other hand, overflows on the sewer network in the Sjölunda catchment area, which depend on how much it rains, the rain intensity, and its duration, amounted to about 252,800 m<sup>3</sup> for 2017, which corresponds to approximately 0.6% of the total wastewater flow to Sjölunda (VA Syd, 2017) (including the flows from the other basins connected to the plant and not just those from Malmö).

### **Climate and precipitation**

Malmö has a temperate climate, experiencing more intense precipitation during summer when approximately 85% of the heavy precipitation events occur (Gustafsson, *et al.*, 2010). The maximum hourly rainfall is 26.1 mm for a 10-year return period and 53.4 mm for a 100-year return period (Hernebring *et al.*, 2015). The mean annual precipitation is 605 mm (Sörensen and Mobini, 2017). The year 2017 was considered a wet year, with about 15% more precipitation than normal annual rainfall (VA Syd, 2017). The rainfall data was obtained from one of the gauges of the SMHI, where the precipitation was recorded at an automatic measuring station every hour. Figure 3.7. shows the location of the rain gauge where the precipitation data was obtained.

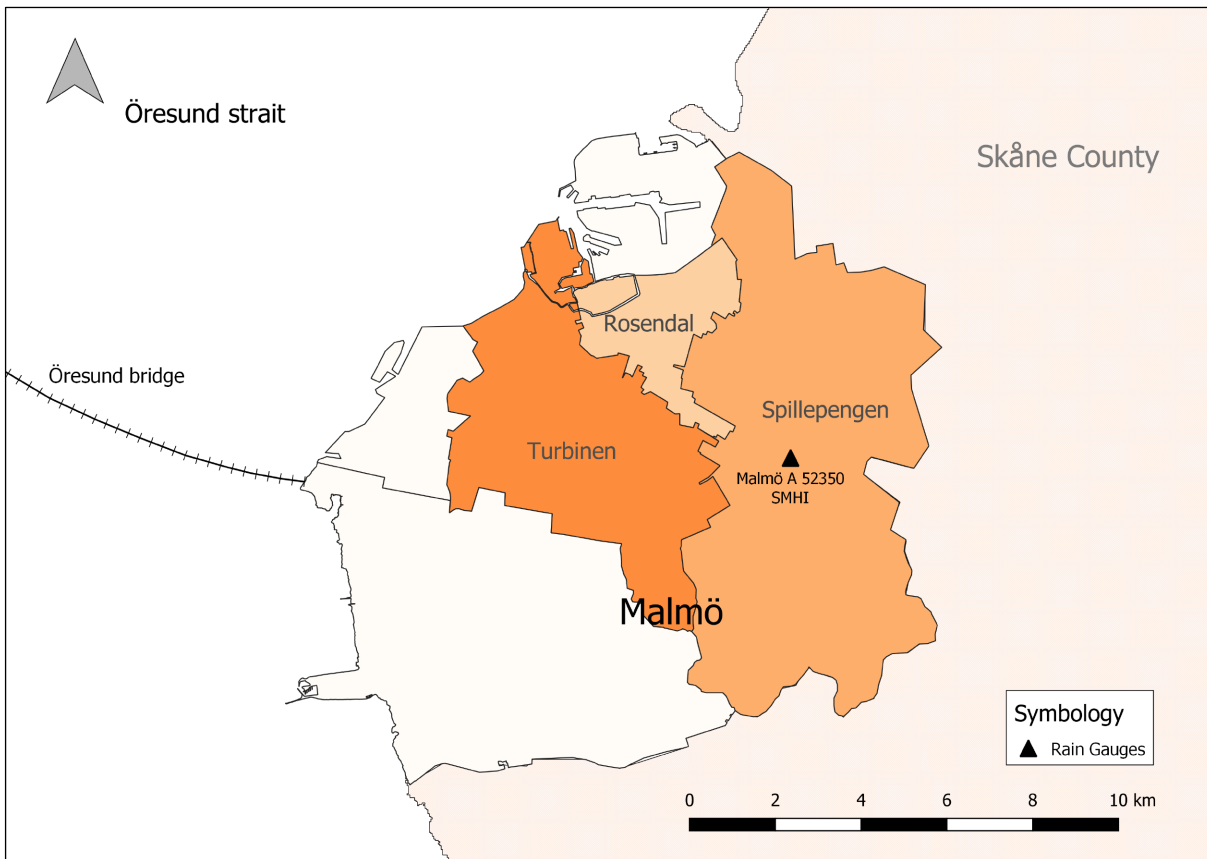


Figure 3.7. Location of the rain gauge where the precipitation data was obtained (A52350 from the SMHI).

### 3.2 Process of modeling the temperature dynamics in the sewer system at a city-wide scale in Malmö

The process of modeling the temperatures in the sewer system utilized measured and existing field data. The use of an existing heat transfer model allowed for estimating changes in the wastewater temperature in different places in the sewer network. The first part of this process involved modeling the changes in temperature in the pipes. After modeling the natural changes in temperature in the pipes, the model was used to estimate the heat recovery potential.

#### 3.2.1 Modeling temperature variations in the sewer system

The modeling process for the temperature variations in the sewer system started with an existing model that followed the heat transfer phenomena described in Abdel-Aal *et al.*, (2014). The model included added components to develop an improved one-dimensional heat transfer model for sewer pipes, where the temperature variations and flow rates were described using a sewer network model developed in MATLAB/Simulink (Saagi *et al.*, 2019). Three main phenomena describing temperature dynamics in the sewer system were included in the model:

1. Convective heat transfer between the wastewater and the in-sewer air in gravity sewer.
2. Heat transfer between the wastewater and soil, through convection between the wastewater and the sewer pipe wall, and conduction from the wastewater near the inner sewer pipe wall to the soil through the pipe.
3. Heat gain due to biological activity.

The overall heat balance equation for each sewer pipe in the model was defined as:

$$mc_p \frac{dT(t)}{dt} = mc_p(T_{in} - T) - q_{Wa}(t) - q_{Ws}(t) + q_{COD}(t) \quad (1)$$

Where  $m$  is the mass flow rate [kg/d],  $c_p$  is the heat capacity of water [J/kg],  $t$  is the time [days],  $q_{Wa}$  is the heat flux between the wastewater and the in-sewer air,  $q_{Ws}$  is the heat flux from wastewater to sewer pipe inside to soil,  $q_{COD}$  is the heat gain due to COD degradation,  $T_{in}$  and  $T$  are the input and output temperatures [K], respectively.

The input data to the model included temperature measurements in Celsius degrees, taken every five minutes during a two-week period in March 2019. The measurements were taken in different parts of the sewer system and flow measurements in  $m^3/d$  were also taken in the same locations and over the same period. The latter measurements were obtained from VA Syd. Both temperature and flow data were labeled as Upstream and Downstream for the different modeling experiments that were carried out for this study. Afterwards, the characteristics of the system were also used as inputs for the model and for calibration of the different parameters the model works with. After an extensive calibration process, a set of parameters, shown in the Results section of this thesis, allowed for small differences between the modeled and the field measured values. Figure 3.8. shows a graphical representation of blocks of the heat transfer model between the PSs and the WWTP.

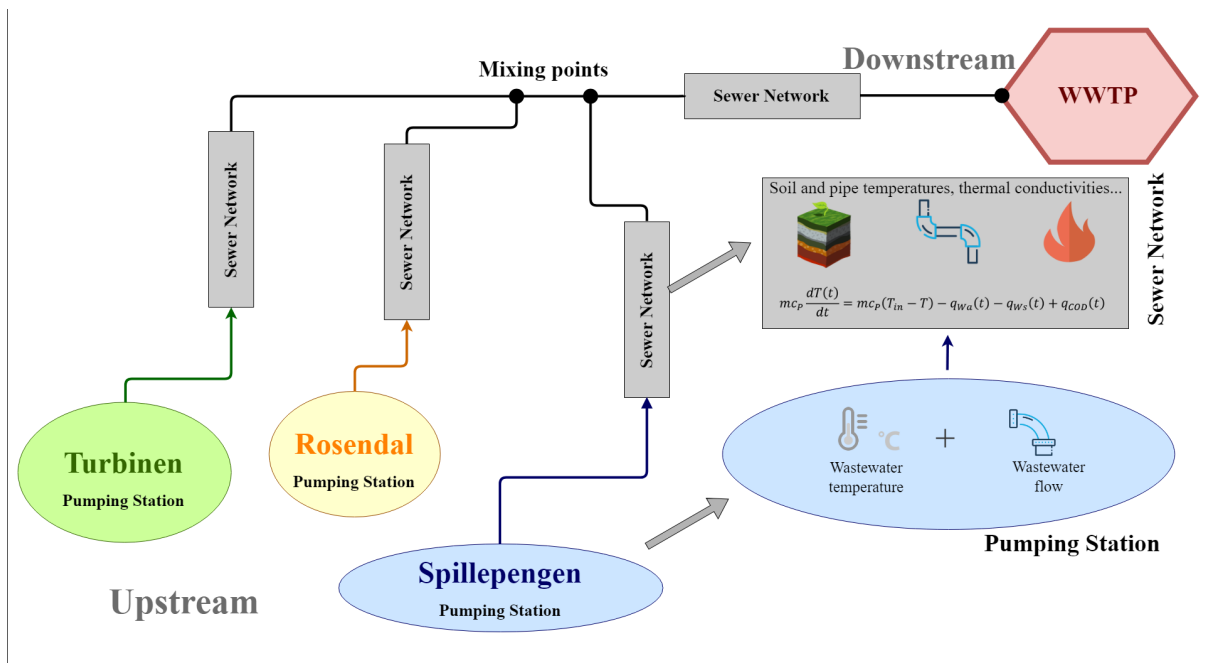


Figure 3.8. Graphical representation of blocks of the heat transfer model.

The temperature modeling process was conducted in three parts:

- M1.** Modeling the wastewater temperature changes in a pipe stretch in Linköping, Sweden, where the model was modified in order to obtain more accurate results following the discovery of a pipe wall-wastewater interaction during the research process of this thesis.
- M2.** Using the upgraded model to determine the wastewater temperature at the downstream end of the 1.6 km stretch in Malmö.

**M3.** Modeling the wastewater temperature changes between the three studied pumping stations and the WWTP (Sjölunda) in Malmö.

### 3.2.2 Modeling heat recovery from the sewer system

The changes in temperature at the downstream ends of the pipes under study were estimated using the following equation to estimate the amount of heat recovered from the wastewater:

$$\Delta T = -\frac{\varphi}{C_p * \rho * Q} \quad (2)$$

Where  $\Delta T$  is the change of the wastewater temperature at the site of extraction [K],  $\varphi$  is the amount of heat recovered from the wastewater per unit of time [J/s] or [W],  $C_p$  corresponds to the specific heat capacity of water [J/kg K],  $\rho$  is the density of water [kg/m<sup>3</sup>], and  $Q$  the discharge of wastewater [m<sup>3</sup>/s]. The dimensional analyses of this equation yields the decrease of the wastewater temperature in K.

The equation was used to determine the temperature changes at the upstream ends of the two stretches studied: the 1.6 km pipe stretch and the stretch between the pumping stations and the WWTP. For example, the decrease in the wastewater temperature,  $\Delta T$ , was determined using the temperature and flow data at every upstream end at the same time interval of the original collected data (5 minutes). The calculations were carried out using Microsoft Office Excel and the new temperature upstream after the extraction of heat was used as an input for the heat transfer model along with the flow data for the same place. Different amounts of heat recovered were studied at different places to determine how the extraction was affecting the temperature of the wastewater at the downstream ends, where the amounts extracted were determined by using  $\varphi$  as a variable and setting a decrease in temperature in K:

- S1.** An estimation of the wastewater temperature at the WWTP after extracting 6,000 kW, 12,000 kW, and 18,000 kW of heat energy.
- S2.** An estimation of the wastewater temperature changes at the end of the 1.6-kilometer stretch after extracting 500 kW of heat energy.
- S3.** An estimation of the wastewater temperature at the WWTP after extracting 18,000 kW of heat energy using the calibrated flows model and similar temperatures to those gathered from the measurements.

The last in the list (S3), the combination of the City-wide model of the sewer flows and the City-wide heat transfer model for the sewer system, was done with the objective of creating a scenario with assumed wastewater temperatures for the pumping stations and their respective modeled flows using the previously calibrated flow model for the city.

### 3.2.3 Characteristics and data measurements from the stretches under study

#### *Characteristics of the 1.6 km pipe stretch in Malmö*

A 1.62 km pipe stretch within the Turbinen catchment, with a diameter of 0.4 meters, was selected for the modeling process. It was chosen because it is an almost closed pipe from end to end (except for just three adjacent pipelines connected to it), which helps maintain the integrity of the modeling process because it limits additional flows into the pipe. This stretch was in a fully residential area and only transported wastewater from the separate system, which means that only wastewater from the households was transported by it and the only addition of water



was by the infiltration in the sewers. Along the stretch, three points were selected as measurement points: the upstream end (well SNB 2427), the downstream end (well S600) and an intermediate point closer to the upstream end (well SNB 2417). The data from the well S600 was obtained from VA Syd for both flows and temperature parameters. The data from the wells SNB 2417 and SNB 2427 was obtained by field data collection with the respective equipment installation process described in this subchapter. The location and scale of the pipe stretch, and the wells are shown in Figure 3.9.

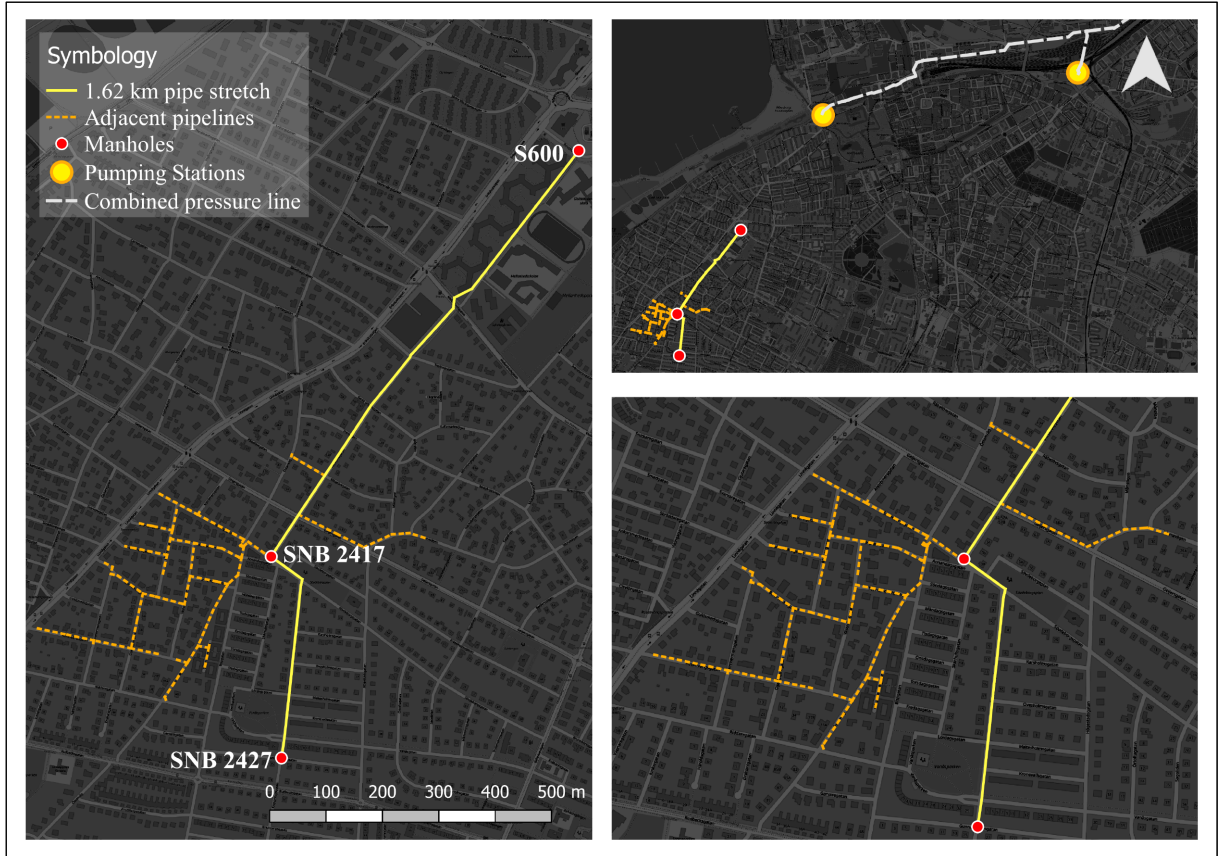


Figure 3.9. Location and scale of the pipe and the wells along the stretch (background map from © OpenStreetMap contributors)

### **Characteristics of the sewer system between the pumping stations and the wastewater treatment plant**

The stretch between the pumping stations and the WWTP was more complex than the single pipe stretch from the previous section because it integrates the wastewater flows from the three catchments and there was a lack of temperature data from the inlet to the wastewater treatment plant. For that reason, temperature measurements from the aeration basins of the biological process were obtained as auxiliary data. The modification of the model to allow for the integration of the flows from the three pumping stations, consisted of adding blocks and equations to sum up flows and calculate the mixing of temperatures depending on the flows from the different pumping stations. The equation used to obtain the temperature of mixed wastewater was:

$$t = \frac{m_1 * t_1 + m_2 * t_2 + \dots + m_n * t_n}{m_1 + m_2 + \dots + m_n} \quad (3)$$

Where  $t$  is the final temperature [K], and  $t_n$  to the temperature of the mixing waters [K].

This stretch consisted of several pressurized pipes with different diameters and lengths. The pipes started at every pumping station, with Turbinen PS farthest upstream and Sjölanda at the downstream end. The other two pumping stations were located between those two and were taken as upstream conceptual blocks within the model. The pipes' diameters ranged from 800 mm to 1600 mm, with a big portion within the 1200 mm and 1600 mm values. The temperature data from the pumping stations was taken during the data collection campaigns described in Section 4.4. and the flow data from those locations, along with the temperature and flow measurements for the WWTP, was obtained from VA Syd. The data received from VA Syd was processed in order to have it organized with the same units and time steps of that collected during the data collection campaigns. The location, scale, and diameter dimensions of the pipelines connecting the pumping stations and the WWTP are shown in Figure 3.10.

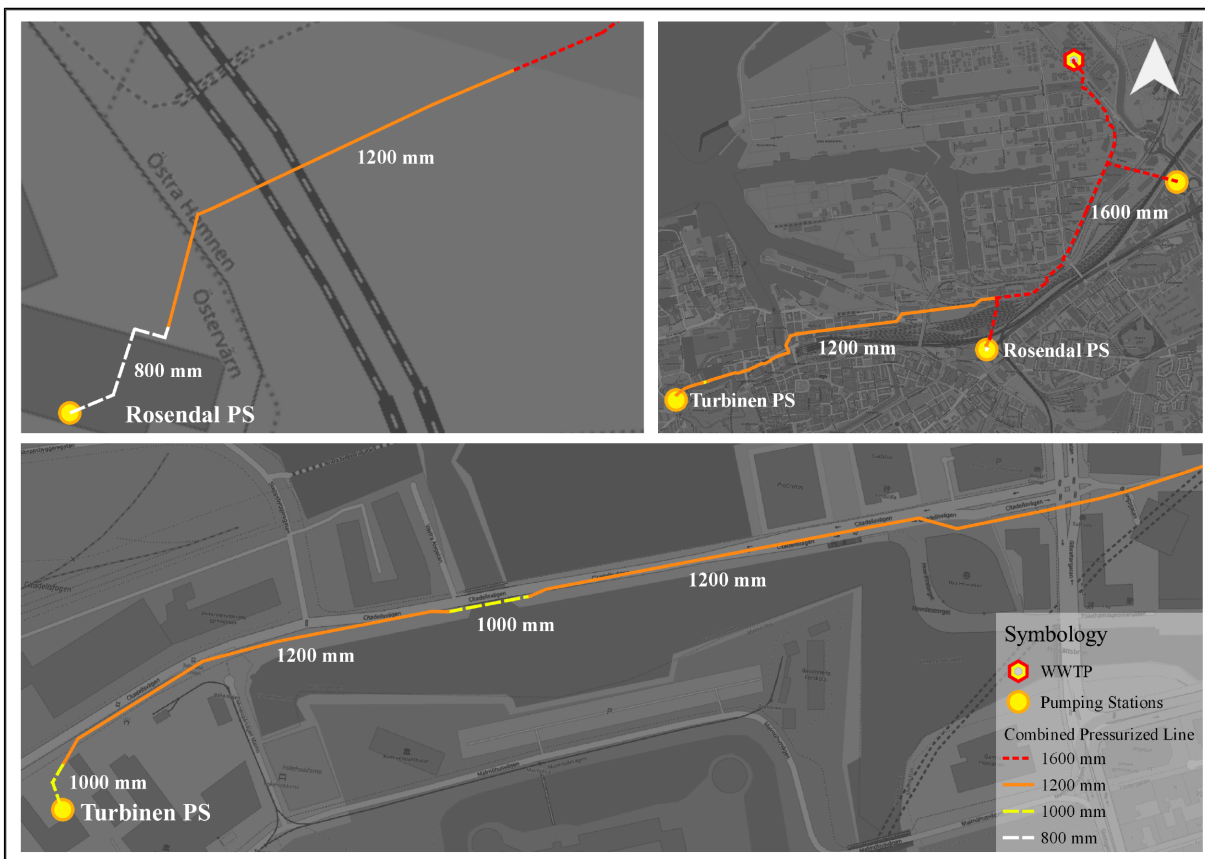


Figure 3.10. Location, scale, and diameters of the pipelines connecting the PSs and the WWTP (background map from © OpenStreetMap contributors). The protanomaly, deuteranomaly, and tritanomaly safe version can be found in Figure 0.6.

### **Installation of equipment and the collection of field data**

The installation of the necessary equipment to measure the wastewater temperature was completed over three planned visits. The locations were selected because of an interest in collecting the data where flow measurements were also available. The selected places included: Turbinen PS, Rosendal PS, Spillepengen PS, Strandshems PS (which was not included in the modeling process because of the fully industrial activity of its catchment), well SNB 2417, and well SNB 2427. The visits were completed collaboratively by researchers from Lund University and representatives from VA Syd.

### Equipment

The instruments used to measure the wastewater and air temperature in the sewer system in Malmö included:

- Temperature data loggers (Tinytag Plus 2 TGP-4020), with the ability to log temperatures from -40 to +125 °C using a thermistor probe. The loggers are waterproof (IP68).
- Encapsulated thermistor probes with a 10-meter cable (PB-5015-10M), which monitors temperatures from -40 °C to +105 °C, flexible and waterproof.
- EasyView software for the management of the data from the data loggers.
- A USB cable for configuring and downloading the loggers and the data from them.
- Computer with Microsoft Windows 10 OS.
- Plastic ties to fix the loggers to any secure structure above the water level.
- Electrical tape to fix the probe's cable nearby the location of the loggers.
- Metal weights to give verticality to the probe's cable and always keep the sensors underwater.

### Installation process

The sensors were installed using the lessons learned from another installation attempted by Dr. Magnus Arnell, project manager at RISE, in Linköping; a place where a similar study was being done when this study began. For the study in Malmö, where four pumping stations and two manholes were selected to install the equipment, different challenges emerged due to the differing types of infrastructure with which each place was equipped (even though the infrastructures have similar functions in the sewer system). For example, Rosendal PS provided a more stable water level than Spillepengen PS and Turbinen. Similarly, well SNB 2427 had only one channel of flow, but well SNB 2417 was an intersection of two flows.

The temperature sensors were located approximately 0.2 meters under the water surface in the pumping stations and about 0.1 meters under the water level in the manholes. The temperature sensor for the air measurements were located about 0.25 meters over the water surface in the well SNB 2417. The log tables created for the first two visits are presented in the Appendix section. The corresponding date for the installation was on March 8, 2018.

### Collection of data

The collection of the measured data during the two-week period was significantly less time-intensive compared to the installation process. This was due to the straightforward procedure to collect the data from the sensors. Collecting the data from the loggers took approximately 3 hours every visit, most of which was transportation time between various logger locations. The data was obtained from the loggers through a USB cable connected from each logger to a computer. The loading time from the loggers was usually a few seconds and the data was immediately displayed on the computer screen. This allowed for immediate diagnosis of the measured data. For example, in Turbinen, the graph display was noisy where the logger was found out of the water at the first interval of data collection. This caused concern until the Rosendal PS data was gathered. In that location, the graph was smoother and more cyclical, like the data collected from other sites. Figure 3.11. shows some of the photos taken during the installation and collection of data processes.



*Figure 3.11. A. Protection of the sensor's cable against rat's bites; B. Data collection in the well SNB 2417 using the computer and the logger; C. Intersection of two flows in the well SNB 2417; D. Inflow basin at Rosendal PS; E. Sensor at Turbinen PS with the metal weight.*

## 4 Results and Discussion

The results from the different processes executed during the project included estimations of flows in the three pumping stations through a calibration process, estimations of the temperature changes in the 1.6 km pipe stretch, between the pumping stations and the WWTP, and estimations of the temperature changes in the sewer system after heat recovery. Also, the temperature measurements taken during the project are shown and analyzed in this section.

### 4.1 Modeling the flow rate dynamics in the sewer system at a city-wide scale in Malmö

#### 4.1.1 Modeling the Catchment and Sewer Network sub-models

##### *Domestic generation*

The daily profiles for the three catchments that better fit the measured daily variation obtained from two years of flow measurements in the pumping stations are shown in Figure 4.1. Coincidentally, the three catchments shared the same daily variation profile, even though every catchment was analyzed separately according to the measured two-year flow data. Likewise, the weekly profiles, which are shown in Figure 4.2., were modified (although to a slightly lesser degree than the daily flow profiles) and graphically followed the same pattern that was proposed in Saagi *et al.* (2016). Regarding the yearly profiles, there was no modification because the original model suggested a 3-week holiday period with a visible reduction in flows from the households during that time.

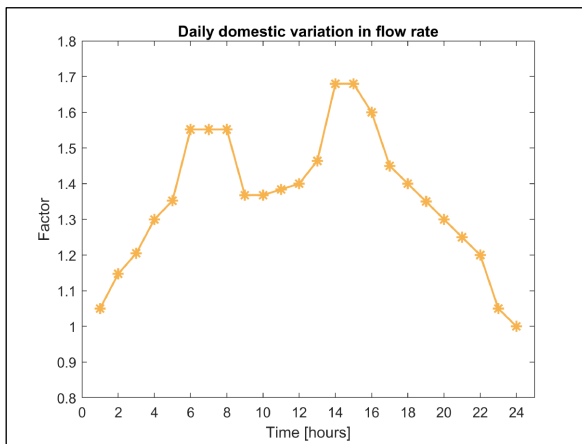


Figure 4.1. Daily profiles for the three catchments that better fitted the measured variation.

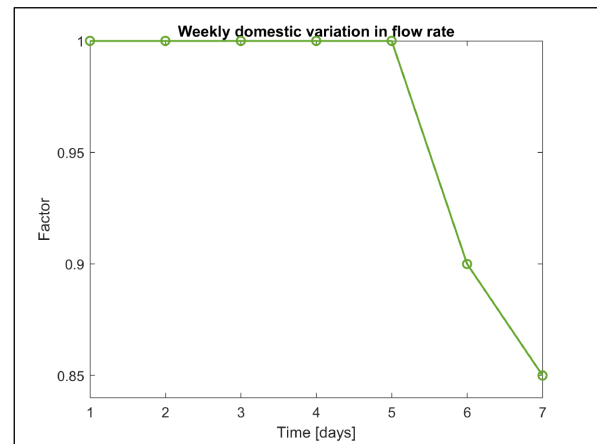


Figure 4.2. Weekly profiles for the three catchments that better fitted the measured variation.

For the Catchment sub-model, the Population Equivalents (PE) for every catchment were determined using a linear relationship between the area of the catchment and the total population of the city. The values were slightly modified to meet the field values obtained from the two-year measurements because there was no data for the population for each catchment. Thus, the numbers related to the PE for each catchment were finally set to 85,000, 80,000, and 160,000, for Rosendal, Spillepengen, and Turbinen, respectively. These numbers sum up the real population of the city connected to Sjölanda.

### **Stormwater generation**

The rainfall data obtained from the SMHI in mm/h is shown in Figure 4.3. The data was taken directly from their website and was not processed other than to transform it to make it available in MATLAB. This process facilitated its introduction into the model because it converted it into the same units as the input data needed for the model. Figure 4.4. shows the total sum of the pumping stations flows. The data was obtained directly from VA Syd and passed through a unit change process to display it in m<sup>3</sup>/d. That figure shows that the flows follow the trends in precipitation displayed in Figure 4.3. and portrays the two most significant changes which were attributable to precipitation during the summer months for both years. Also, the rainfall data confirmed that 2017 was a wet year compared with 2018. Lastly, data from the SMHI fit better with the historical values than that received from VA Syd. Thus, this data was used as it resulted in better accuracy during the model calibration.

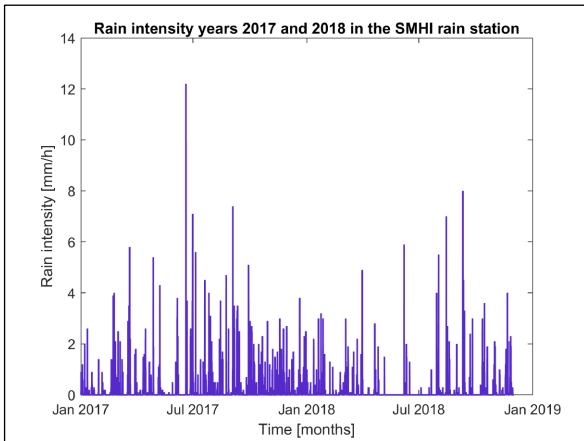


Figure 4.3. Data from the SMHI in mm/h.

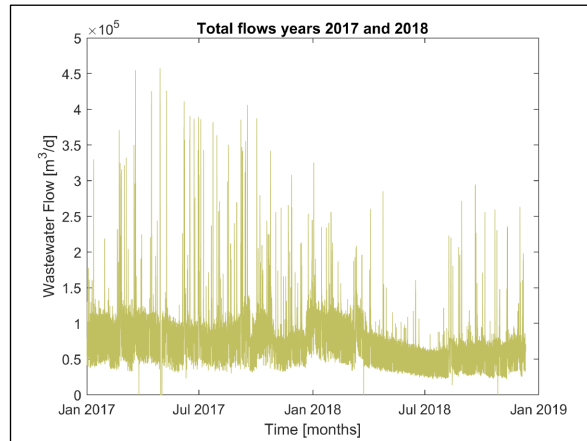


Figure 4.4. The total sum of the PS's flows.

### **Infiltration to sewers**

In this part, the assigned infiltration value was 30,000 m<sup>3</sup>/d, which corresponded to infiltration of 30% of the total inflow to Sjölanda (matching actual recorded data for 2017), with an amplitude of 0.4. These values show that the sewer system has a strong influence from the annual groundwater flow variation, which is clearly visible in the sinusoidal wave in Figure 4.7. corresponding to the measured and modeled flows for Spillepengen. Additionally, the phase of the sinusoidal wave (that can be defined as the horizontal movement of the curve along the horizontal axis) needed to be modified to match the catchments behavior with a value of  $\frac{5\pi}{12}$ .

The different parameters used to model the flows in the pumping stations using the BSM-UWS model were calibrated based on catchment characteristics and other data (flow rate profiles at pumping stations etc.) from Malmö. For example, the PE, the percentage of impervious areas of every catchment, the daily, weekly, and yearly variation profiles of flows, the percentage of infiltration to the sewer system from the ground and its seasonal variation, and the areas in the city connected to the pumping stations, among others that are presented in Table 4.1. The results from the modeling process are shown from Figure 4.5. to Figure 4.9. The numbers 1, 2, and 3 correspond to Turbinen, Rosendal, and Spillepengen, respectively.

Table 4.1. Parameters used for the calibration of the flows model for the three catchments.

Parameter	Definition	Value	Unit
QperPE	Domestic wastewater production per inhabitant per day	0.18	m <sup>3</sup> /PE*day
PE1	Population Equivalents for domestic wastewater	160,000	PE
PE2		85,000	
PE3		80,000	
Area	Total area of the built system in the city (combined + semi-separate + separate systems)	4,722	ha
a1	Percentage of area that is managing combined flows (affected by precipitation events)	0.205	ha
a2		0.117	
a3		0.061	
Imp-frac1 Imp-frac2 Imp-frac3	Impervious fraction of the sub-catchment.	0.6	-
gwbias	Mean input flow rate to the infiltration model.	30,000	m <sup>3</sup> /day
amp	Amplitude for the gwbias parameter for each sub-catchment.	0.4	-

Figure 4.5. shows the result of introducing into the model precipitation data in mm/d from the SMHI, along with the parameters presented in Table 4.1.. In that figure, the seasonal sinusoidal variation of flows is followed by the model for the two-year period and the peaks have a close connection between the model and measured values (suggesting that the fit between those two is good). Figure 4.5. also confirms that 2017 was a wet year and, for that reason, in the modeled plot there is an underestimation of flows in 2017 and an overestimation of flows in 2018. This singularity can be explained by the fact that in that figure the plotted flows are the sum of flows for the three catchments, which have different percentages of the combined and separate system and affect to different magnitudes the estimation of flows.

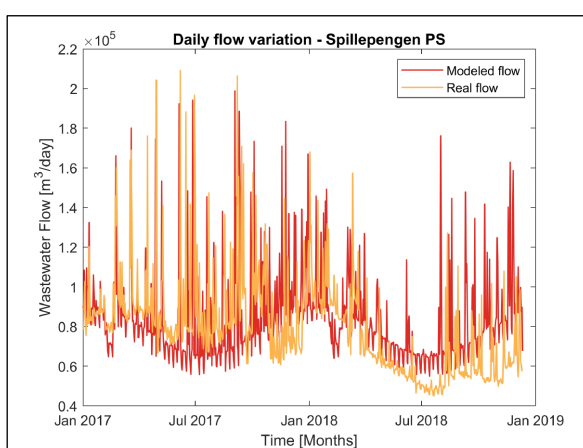


Figure 4.5. Modeled and measured flows for all the PSs using precipitation data in mm/h.

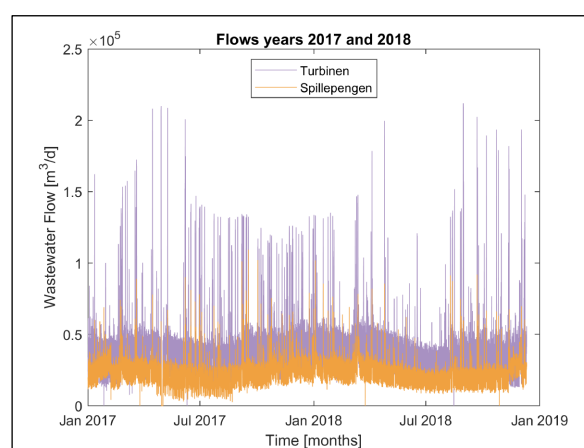


Figure 4.6. Flows in Turbinen PS and Spillepengen PS (years 2017 and 2018)

Analysis suggests that Spillepengen, the biggest catchment in the area, presented the most ideal scenario to model dry weather flows, due to the low percentage of combined systems (13%). As can be seen in Figure 4.6., Spillepengen was less influenced by precipitation events, which means, lower peaks in wastewater flow than the other two catchments. In the figure, it is only

compared with Turbinen because that catchment showed more similar values for the peaks than Rosendal, although Rosendal has a smaller area than Turbinen. This was due to Rosendal's significant percentage of combined system (85%), which create greater flows towards the pumping stations when precipitation events occur.

The low percentage of combined systems for Spillepengen directly translated to the plotted measured and modeled flows: when precipitation events occurred, the peak values for flows were close to the average value, allowing for a clear visualization of the seasonal variation of flows (during the summer months there was a decrease in the infiltration to the sewer system and peaks occurred in winter, when humidity in the soil is usually constant and snowmelt events occur). The amplitude of the yearly variation curve, which followed a sinusoidal shape, was around 0.4, allowing for an almost perfect fit with the actual variation of the yearly infiltration from groundwater sources. Additionally, where dry weather was present, daily patterns could clearly be observed. Figure 4.7. shows the real and modeled flows for Spillepengen.

Finally, mismatching flows between the measured and the modeled flows in Figure 4.7. may have occurred because the volumes for the storage basins were not included in the model. However, the estimate generated with the BSM-UWS model showed close relationship between measured values in both wet and dry weather using measured parameters from the catchments. The difference between the model and the measured values for Spillepengen during dry periods was in average 200 m<sup>3</sup>/day, which corresponds to 1% of its average daily flow.

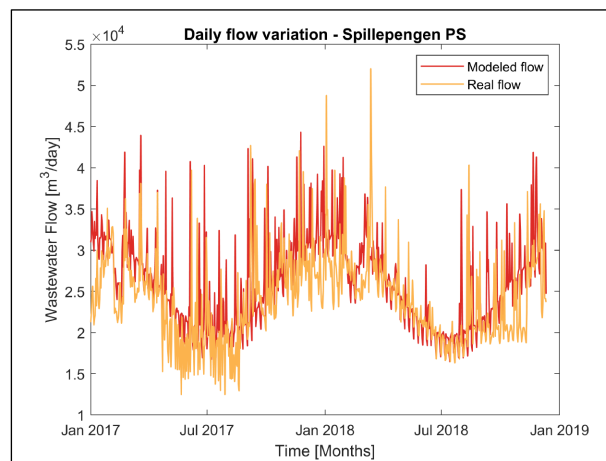


Figure 4.7. Modeled and measured flows at Spillepengen PS during a two-year period.

On the other hand, the modeling process for the other two catchments presented more complexity due to the variations in wet weather flow rate because of the catchment's high ratio of the combined system. For example, Rosendal, the smallest catchment in terms of area and in terms of built sewer systems, but with an 85% ratio of the combined system, had extreme peaks when precipitation events occurred (peaks twice as big as the average annual value during 2017). Additionally, the measured flow data from this catchment presented some noise and null values that hindered the modeling process. Nevertheless, the relevant period for this study, corresponding to dry weather, presented smaller differences between the modeled and measured data for the year 2018. There, the real seasonal variation due to infiltration from groundwater was accurately described by the model and the peaks from precipitation events were almost equaled by the model. The difference between the model and the measured values for this catchment during dry periods was, on average, 1,000 m<sup>3</sup>/day, which corresponded to 4% of its average



daily flow. The plot for both data sets is presented in Figure 4.8., where the year 2018 was the focus for the analysis due to the lesser influence by precipitation events.

Similarly, the model results from Turbinen followed, to some extent, the measured values. Although some of the results deviated because this catchment had half of its built system as a combined system and was the catchment with the greatest population. For example, the model result showed an overestimation during 2018. However, for this case, the wet weather peaks for both years were similar for the model and the measured values, which may indicate that the model was able to determine flows during wet weather in catchments where half of its area consists of a combined system (contrary to Rosendal). The seasonal variation is also visible in the results from the modeling process. The difference between the model and the measured values for this catchment during dry periods was, in average, 4,000 m<sup>3</sup>/day, which corresponds to 10% of its average daily flow. The plot for both modeled and measured flows for the 2017 – 2018 period is shown in Figure 4.9.

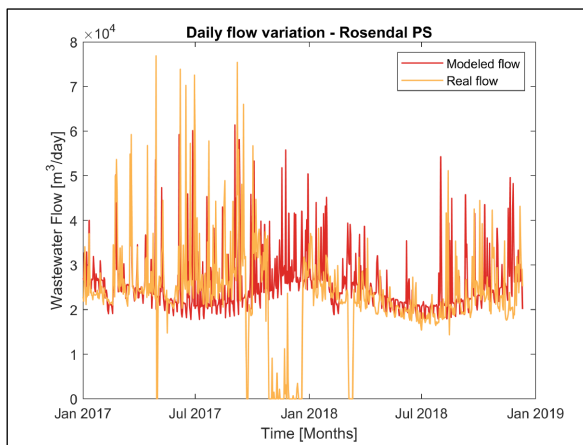


Figure 4.8. Modeled and measured flows at Rosendal PS during a two-year period.

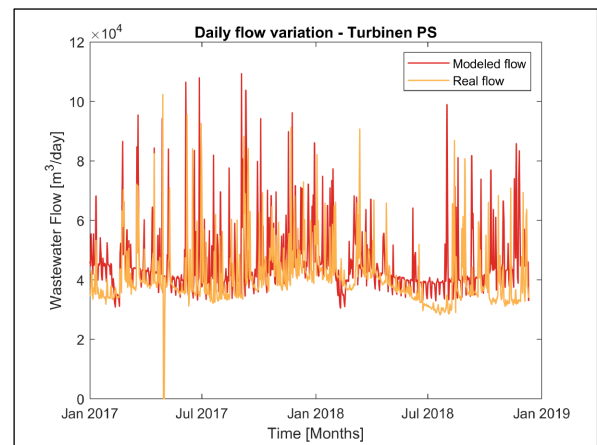


Figure 4.9. Modeled and measured flows at Turbinen PS during a two-year period

## 4.2 Modeling the temperatures dynamics in the sewer system at a city-wide scale in Malmö

### 4.2.1 Analysis of field data

The results from the collection of field data are shown in Figure 4.10. to Figure 4.17. In all the figures, there is a clear trend of higher temperatures during the day and lower temperatures during the night. That effect is produced by the amount of wastewater that reaches the sewer system and is explained by the daily variations of wastewater from the households shown in Figure 4.1. It was also observed that the wastewater temperature presented fewer lower peaks as a result of lessened influence by precipitation events. Figure 4.10. shows the temperature variation for Turbinen PS in the two-week period. There, the average temperature was approximately 12 °C, which is the lowest average for the three pumping stations measured and studied in this project. Similarly, it presented an average daily maximum temperature of 13.5 °C and daily minimum around 10.2 °C, demonstrating a difference of 3.3 °C between the night and the day peaks. Additionally, for Turbinen PS, the location of the sensor was in a basin where the inlet water was mostly from the separate system, suggesting that even during precipitation events the temperature changes did not vary extremely compared with the normal daily changes in temperature in that pumping station. That was demonstrated in Figure 4.10 where, during the precipitation event on March 25, the temperature changes were not more drastic than the rest

of the days. Finally, it is important to clarify that the second data set, corresponding to data from March 19 to March 26, is the most representative one for this pumping station because the sensor was found in the air during the first data collection campaign, which created temperature values up to 16 °C during the first week.

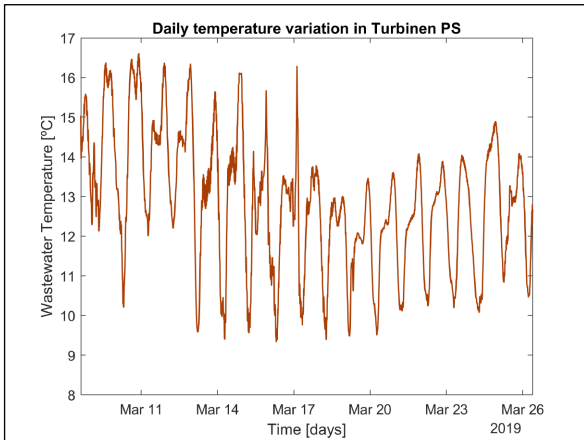


Figure 4.10. Wastewater temperature in Turbinen PS in a two-week period.

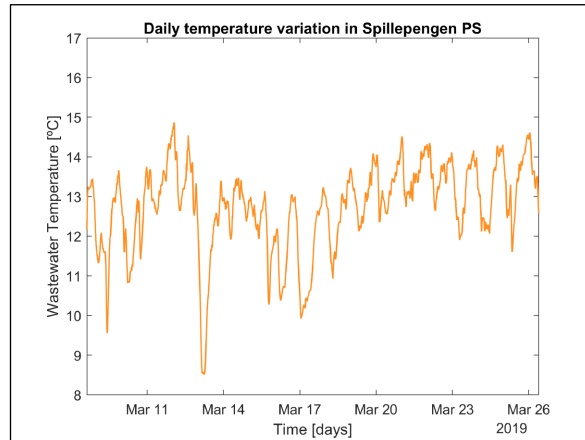


Figure 4.11. Wastewater temperature in Spillepengen PS in a two-week period.

Figure 4.11. shows the daily temperature variation in the Spillepengen pumping station, where the sensor was found located under water in both periods of data collection (which indicated a good representation of the wastewater temperature in that place). During the second week of temperature recordings, the daily temperature variation showed the expected cyclical changes with a reasonable amplitude between night and day, where those changes were between 12.5 °C and 14 °C, respectively, resulting in a difference of 1.5 °C. However, in the first week, like in the rest of the places in the city, the temperature was influenced by the precipitation events that occurred constantly during that time. During that period, the wastewater temperature fluctuated more significantly between the lower and higher peaks. Also, the comparison between the changes when precipitation events occurred, in Turbinen PS and Spillepengen PS, showed that the latter was more influenced in terms of its wastewater temperature, even though it had the biggest percentage of separate system of all the catchments. This may have occurred due to infiltration of groundwater into the sewer network in this catchment and may indicate the physical state of the pipes. The effect of the precipitation events can be observed in Figure 4.11., where peaks reached low values compared with the average temperature. Also, it can be said that that fluctuations in temperature are bigger when precipitation events occur. For example, the lowest values for Spillepengen PS occurred during the strongest precipitation event on March 13. After that, another two precipitation events influenced low temperatures. Subsequently, at the beginning of the second week, a stabilization of the wastewater temperature variation was observed due to the dry conditions for that period.

Like the data for the other two pumping stations, the data from Rosendal PS showed drastic changes during precipitation events (the first week), but for the second week, a less varied curve was obtained. However, at this pumping station, there was an extremely high-temperature peak on March 21, where no precipitation was recorded in the city and the recorded time, 4:00 a.m., did not suggest a conclusion related with daily temperatures. When the big precipitation events occurred, however, lower temperature values happened in this pumping station, as was the case in the other pumping stations. This suggests again that wastewater temperature changes are more susceptible when precipitation events occur. During the second week, the

average higher temperature, which corresponded to the daily measurements, was around 17.1 °C, and the same measurement but for the night was around 14.2 °C, resulting in a difference of 2.9 °C between the night and day. Figure 4.12. shows the information gathered at Rosendal PS. For an understanding of the relationship between the wastewater temperature and the precipitation events, Figure 4.14. shows the precipitation intensity for the two-week period.

For the wastewater temperature measurements in the 1.6 kilometer stretch in Malmö, the two measured wells at the upstream end of the stretch presented very similar temperature changes during the day and night. Also, due to the stretch characteristic of only conveying water from the separate system, the changes in temperature when precipitation events occurred did not influence the graph as drastically as in the pumping stations. Finally, Figure 4.13. shows the similarity between the temperature in both wells. Because of this, well 2427, which is in the most upstream part of the stretch, was selected for the analysis for this study and was labeled as Upstream.

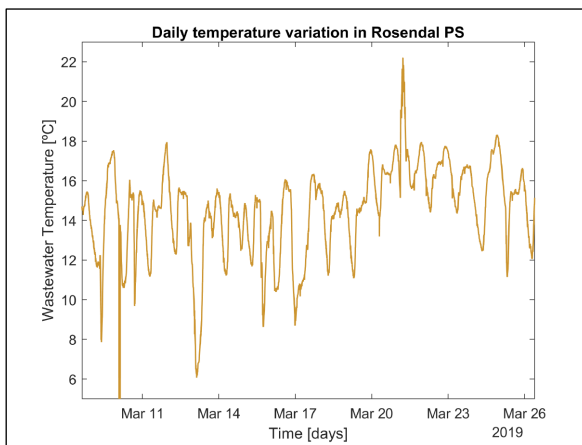


Figure 4.12. Wastewater temperature in Rosendal PS in a two-week period.

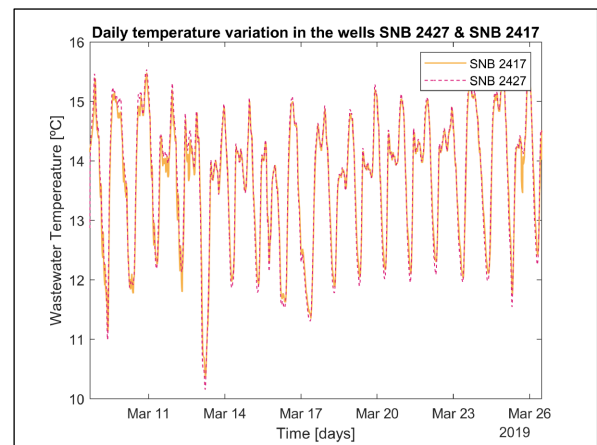


Figure 4.13. Wastewater temperature in the well SNB 2717 and SNB 2427

A comparison was done between the wastewater temperature in well 2427 and the precipitation data from the SMHI gauge in Figure 4.14. In this comparison, a clearer influence of precipitation events in the temperature was observed, even though the water transported by that stretch belongs to the separate system in the Turbinen catchment. This can also explain why for the pumping stations, which have different percentages of combined systems, the precipitation events influenced the temperature of the wastewater to such a significant degree. For example, the strongest precipitation event on March 13th induced a lower peak in that well, but the rest of the graph presented a very similar variation during the whole two-week period. The second-week data set presented an even better representation with less variation of temperature changes due to the dry weather conditions during that time.

Similarly, a comparison done between the temperature of in-sewer air temperature in well 2427 and the air temperature at ground level, the plot displayed in Figure 4.15., shows that the wastewater temperature is always warmer than the in-sewer air temperature and the air temperature in the ground. Also, the in-sewer air is warmer than the air temperature in the ground, which suggests that the wastewater heats the air in the pipes. The warming up process can be seen in the same Figure 4.15., where the in-sewer air temperature follows the same shape of the wastewater temperature and is always warmer than the ground level air temperature. On the other hand, due to the enclosed conditions in the pipes, the influence from the colder ground

level temperature is not as clear as that from the wastewater because the latter is in permanent contact with the air inside the pipe.

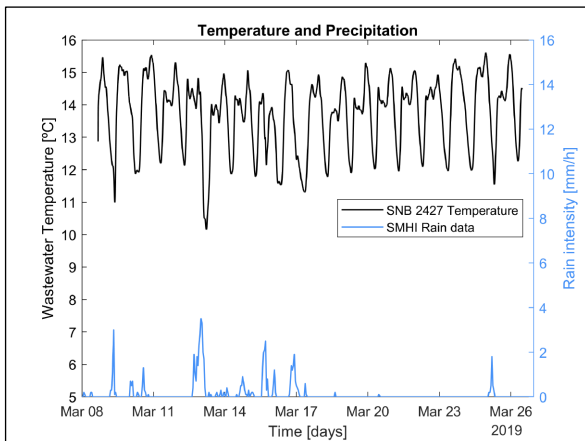


Figure 4.14. Relationship between wastewater temperature and precipitation.

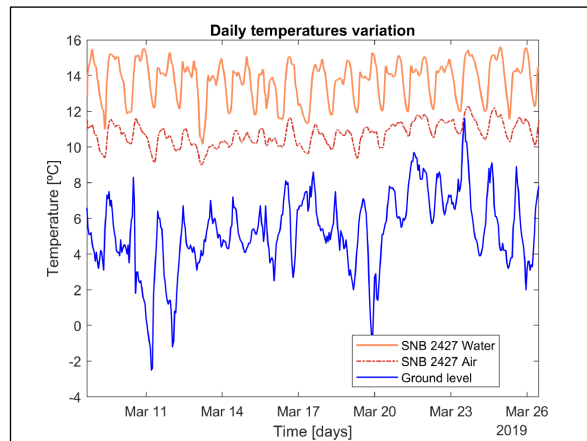


Figure 4.15. Wastewater, in-sewer air, and ground air temperatures in the well 2427.

As expected for this stretch, the wastewater temperature in its downstream end presented a lower value than its upstream end. Though, this only happened during the daytime when the maximum flows from the households usually occur. During the night, from midnight until 6:00 AM in the morning (hours where the water flow decreases from the households) the behavior was different: the downstream temperature was warmer than the upstream temperature. This suggests a warming up process in the wastewater as it moves downstream. Figure 4.16. shows the variation in temperature of the wastewater of the upstream and downstream ends and Figure 4.17. shows a zoomed view of those changes. This phenomenon is explained in Dürrenmatt and Wanner (2014), where the heat stored in the pipe walls can be released into the wastewater as long as the temperature in the wastewater is lower than that of the pipe. In this case, it can be translated as: the measured temperatures show that the pipe wall is accumulating heat from the wastewater during the day and the wastewater is recovering that heat from the pipe during the night. Finally, the graph in Figure 4.17. also shows that there are two peaks of warmer temperature during each day, one in the morning and one in the afternoon. That is likely linked with household activity, where people start activities in the morning and then come back to the houses in the night. This is visible in Figure 4.1.

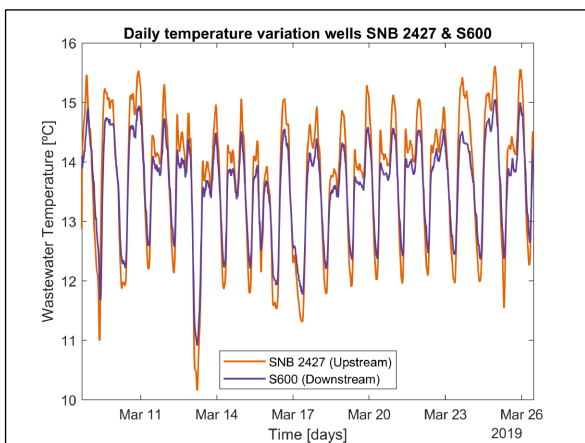


Figure 4.16. Temperature variation at the ends of the 1.6 km stretch.

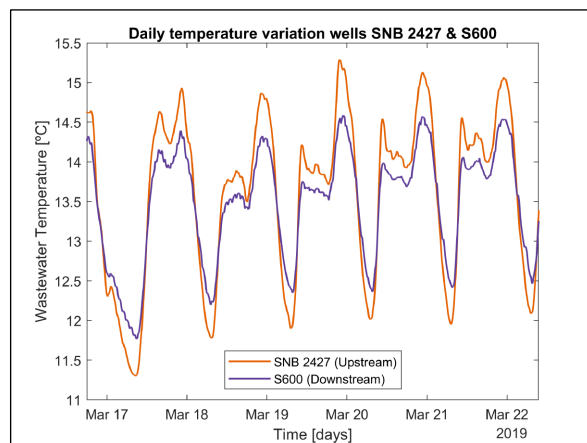


Figure 4.17. Zoomed view of the temperature variation at the ends of the 1.6 km stretch.

#### 4.2.2 Modeling temperature variations in the sewer system

The next step in the project involved the estimation of the wastewater temperature changes at the downstream ends of the different places under study (without conducting any heat extraction from the system yet). Three different models were created and analyzed on this part:

- M1.** Modeling the wastewater temperature changes in a pipe stretch in Linköping, Sweden, where a modification to the model was done in order to obtain more accurate results due to a pipe-water interaction found during the research process of this thesis.
- M2.** Modeling of the 1.6 km stretch in Malmö with the upgraded model to determine the wastewater temperature at the downstream end.
- M3.** Modeling of the wastewater temperature changes between the three studied pumping stations and the WWTP (Sjölunda) in Malmö.

The parameters used for both the 1.6-kilometer stretch and between the pumping stations and the WWTP were the same except for the pipe's characteristics (diameter, length, thickness, and the soil depth for heat transfer). Table 4.2. shows the parameters used in both experiments that are attached to real ranges for each variable.

*Table 4.2. Parameters used for the calibration of the heat transfer model for the three pumping stations and the 1.6 km stretch.*

Parameter	Definition	Value	Unit
<b>Tair</b>	In-sewer air temperature	11	°C
<b>Tsoil</b>	Soil temperature (1.6 km stretch)	13.1	°C
<b>Tsoil</b>	Soil temperature (PSs to WWTP)	12.3	°C
<b>diameter</b>	Pipe diameter (1.6 km stretch)	0.4	m
<b>diameter</b>	Pipe diameter (PSs to WWTP)	variable	m
<b>slope</b>	Horizontal slope of the pipe from end to end	0.002-0.006	m
<b>mannings</b>	Manning's coefficient for concrete pipes	0.01	-
<b>hwa</b>	Heat transfer coefficient wastewater to in-sewer air	1.9	W/m <sup>2</sup> *k
<b>kp</b>	Thermal conductivity of pipe	2.3	W/m*k
<b>ks</b>	Thermal conductivity of soil	5.5	W/m*k
<b>ds</b>	Soil depth for heat transfer (1.6 km stretch)	0.05	m
<b>ds</b>	Soil depth for heat transfer (PSs to WWTP)	0.15	m
<b>wt</b>	Pipe thickness (1.6 km stretch)	0.04	m
<b>wt</b>	Pipe thickness (PSs to WWTP)	0.40	m
<b>ecod</b>	Reaction enthalpy for COD degradation	14x10 <sup>6</sup>	J/kgCOD
<b>rcod</b>	Degradation rate in sewers	1x10 <sup>-6</sup>	kgCOD/m <sup>3</sup> *s

#### **M1. Model improvement using the data from Linköping, Sweden**

While working with the data sets obtained from Linköping, the temperature variations showed the expected cyclic variation. During the day, the temperature was warmer than in the night. However, the same phenomena that occurred with the data from Malmö, where the downstream temperature was warmer than the upstream temperature during the night, also occurred. Additionally, when modeling the temperature changes, it was found that the model could success-

fully represent the temperatures during the day but, during the night, the model under-calculated the temperature. This means that the model was predicting a colder temperature for the downstream end during the night, which, in real life, was not happening. For this reason, a research process regarding soil temperature changes during the day and during the year was conducted to determine if the normal soil temperature variations affected the wastewater temperature. One of the sources concluded that the temperature in the soils that are under a depth of 1.5 meters change very little during the year and that the changes are even smaller in a daily cycle. For example, Florides and Kalogirou (2005) showed that the yearly variation of the soil temperature was very small under depths of 1.5 meters and the daily temperature change was negligible during the day under a 0.5 meter depth.

Linking that finding with some information from Dürrenmatt and Wanner (2014), which showed that the wastewater can be warmed up again from the heat retained by the pipes during the day, a curve describing a variable pipe temperature was created as an input for the model. The curve defined the pipe temperature as a function of the wastewater temperature at the downstream end every hour during a 24-hour period. For example, from measured values, it was discovered that there was a warming up of the wastewater from midnight to approximately 8:00 AM in the morning. For this reason, the factors show a value over 1 (up to 1.0095) from midnight to around 10:00 AM in the morning, and values under 1 (down to 0.985) from 11:00 AM to 11:00 PM, which means that the pipe temperature is going to be warmer than the wastewater from approximately midnight to 10:00 AM in the morning.

The result from this new input (the variable pipe temperature), would allow for heat exchange between the pipe and the wastewater, where the latter will gain temperature from the former. It was also interesting how a small variation on the pipe temperature made an improvement in the model, which suggested how the pipe temperature was a sensitive parameter in the model (this variable temperature was introduced in the model as the soil temperature for testing purposes). Finally, after introducing the variable pipe temperature to the model, as variable soil temperature, a more accurate downstream wastewater temperature was obtained from the model for two different data sets in Linköping. It is important to highlight that this finding and the consequent modification of the model is an important outcome from this thesis because it allowed the model to successfully predict the temperature changes in different pipes sections in Linköping and Malmö. Also, the factors are only used for testing and the model was later upgraded to include a new state variable for the pipe temperature and an energy balance for the concrete pipe. Figure 4.18. shows the factors for the pipe temperature for a 24-hour period.

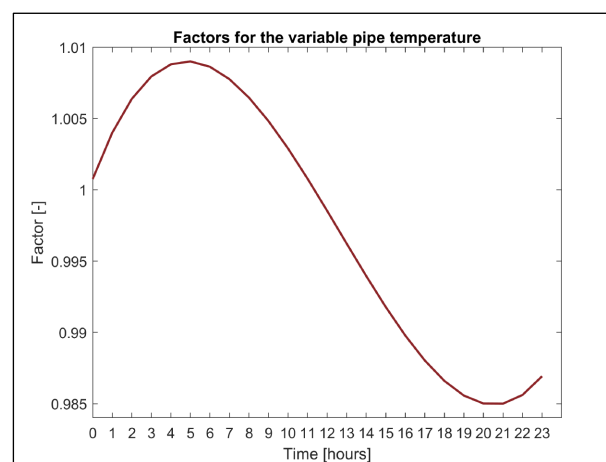


Figure 4.18. The curve defined by the factors for the pipe temperature in a 24-hour period.

The first data set from Linköping was recorded at the end of November 2018 over 7 days. The results from this data set are shown in the appendix section. The second data set from Linköping was recorded at the beginning of February 2018 also over 7 days. The wastewater temperature in the stretch of pipe used in that study, 2.1 km long, was around 7 °C. This data set presented a smooth curve with the expected daily variation and after modeling using the modification for the dynamic pipe temperature, the graphs of the measured values and the model output were very close for both day and night. The results from the original model can be seen in Figure 4.19. and the results from the modeling process using the variable pipe temperature can be seen in Figure 4.20. It is important to note that the differences between the measured values and the model were under 0.5 °C in the original model, and in the improved model, the differences were around 0.1 °C, which is a significant reduction that can clearly be observed by comparing the plots before and after the modification.

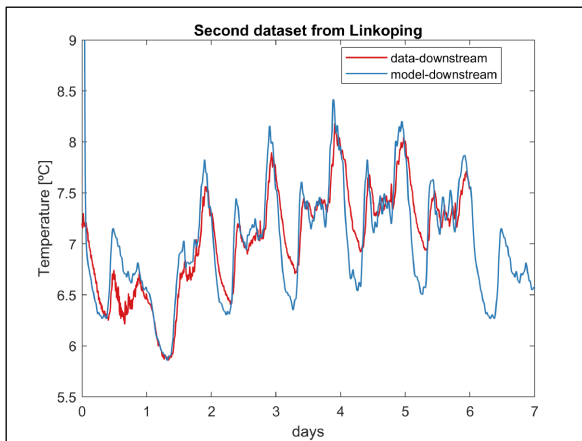


Figure 4.19. Second data set from Linköping using the original model

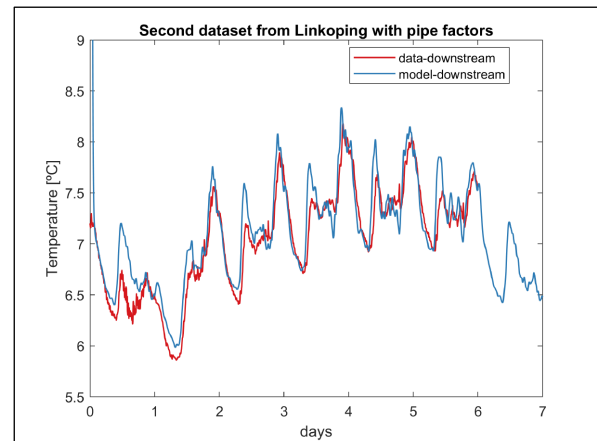


Figure 4.20. Second data set from Linköping using the pipe factors.

Because introducing a variable pipe temperature so significantly improved the model, a modification to the code in the model was introduced by Dr. Ramesh Saagi, with another heat exchange equation. The modification of the model consisted of the introduction of a heat balance for the concrete pipe, which results in a dynamic pipe temperature.

**M2. Modeling of the 1.6 km stretch in Malmö with the upgraded model to determine the wastewater temperature at the downstream end.**

Following the same trend as in the Linköping case, the data from Malmö during the two-week period showed a cyclic variation every day, and during the day, warmer temperatures were recorded than in the night. Though, in the 1.6-kilometer stretch in Malmö, a similar phenomenon occurred during the night as was the case in the Linköping study: The temperature downstream was warmer than upstream.

The results from this new modeling process delivered a very good estimate of the wastewater temperature downstream in both day and night periods with good accuracy (differences between measured and modeled data were between 0.1 and 0.3 °C). This also confirmed the importance of considering the pipe temperature when modeling the wastewater temperature changes in pipes. Figure 4.21. shows the measured and modeled temperatures upstream and downstream in pipes. Figure 4.22. displays the measured and the model downstream temperatures, where the model follows the measured temperature with almost complete synchrony. It is also

important to note that the model uses a few parameters to accurately predict the wastewater temperature changes in the sewer system.

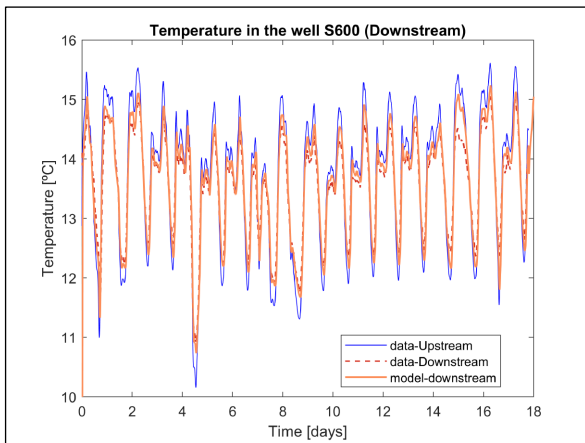


Figure 4.21. Real and modeled wastewater temperature in the Malmö 1.6 km stretch

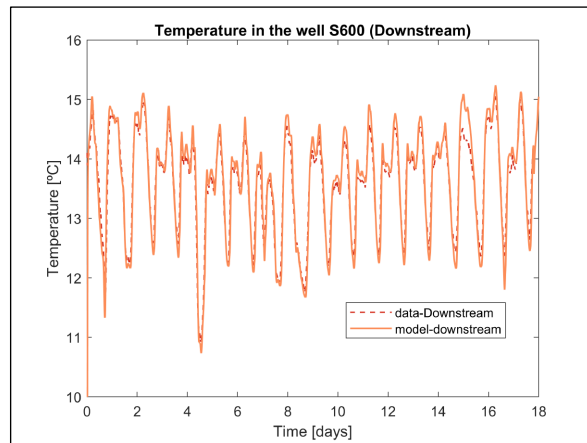


Figure 4.22. Real and modeled wastewater temperature in the Malmö 1.6 km stretch

**M3. Modeling of the wastewater temperature changes between the three studied pumping stations and the wastewater treatment plant (Sjölunda) in Malmö.**

The modeling process in this part focused on obtaining the results at the end of the pressurized pipe to compare them with the measured values from the wastewater treatment plant. First, a comparison between the results of the model upstream and downstream was made to check that there was a decrease in the temperature and that the phenomena that had occurred in both Linköping and Malmö was also happening in that pressurized pipe. For example, in Figure 4.23. the temperature from the model at the downstream end (at the WWTP) was cooler than the temperature upstream (upstream is at the point where the three PS flows mix and flow to the WWTP), except for during the night, where these temperatures were warmer than the upstream end. Next, the measured temperatures at the WWTP and the output from the model at the same place were compared.

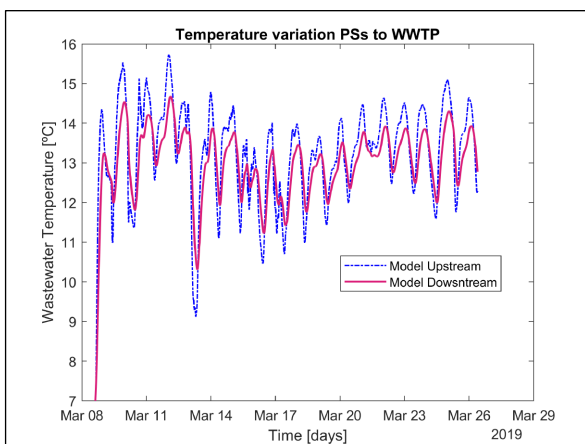


Figure 4.23. Modeled wastewater temperature in the pressurized pipe that connects the PSs and Sjölunda.

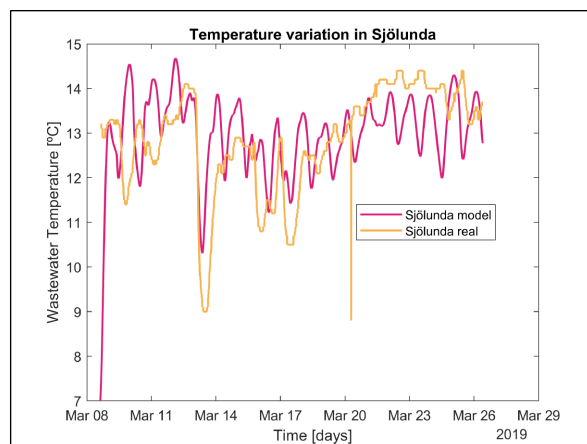


Figure 4.24. Real and modeled temperature at the inlet of Sjölunda.

Figure 4.24. shows that there is a clear relationship between the measured and the modeled temperatures, even though the measured values from the WWTP were not very representative



because they were taken at the aeration basins. However, the closeness of the graphs still suggests that the model can accurately predict the wastewater temperature at this place. Additionally, the drops in temperature occurred almost at the same time in both graphs, and, during the dry week (the second week), the temperature estimated by the model was lower than the measured values, suggesting that internal processes at the WWTP may keep the temperature at higher values. The model predicted the wastewater temperature at the WWTP with an acceptable accuracy, where the differences between measured and modeled data were between 0.1 and 1.2 °C.

#### 4.2.3 Modeling heat recovery from the sewer system

One of the final steps of this project involved estimating wastewater temperature changes at the downstream ends of the different places under study after conducting heat recovery at their upstream ends, assuming ideal heat transfer without any losses when estimating the heat energy available for recovery. This could be done because of the successful calibration process of the heat transfer model, which allowed for the estimation of temperatures at downstream ends of the studied stretches using any combination of flows and temperature data. The three scenarios analyzed in this part showed that the flow of wastewater is a very sensitive parameter that defines how much heat can be extracted from the system. Those scenarios were:

- S1.** An estimation of the wastewater temperature at the WWTP after extracting 6,000 kW, 12,000 kW, and 18,000 kW of heat energy.
- S2.** An estimation of the wastewater temperature changes at the end of the 1.6-kilometer stretch after extracting 500 kW of heat energy using the two-week collected data.
- S3.** A simulation of the wastewater temperature at the WWTP after extracting 18,000 kW of heat using the calibrated flows model and similar temperatures to those gathered from the measurements.

##### ***S1. Modeling heat recovery from the PSs to the WWTP using the two-week collected data***

The first case modeled the changes in the wastewater temperature at the WWTP after extracting different amounts of heat at each pumping stations. The results from the different extractions are shown in Figure 4.25., where the previous modeled wastewater temperature without any extraction is plotted above the rest of the lines for comparison purposes.

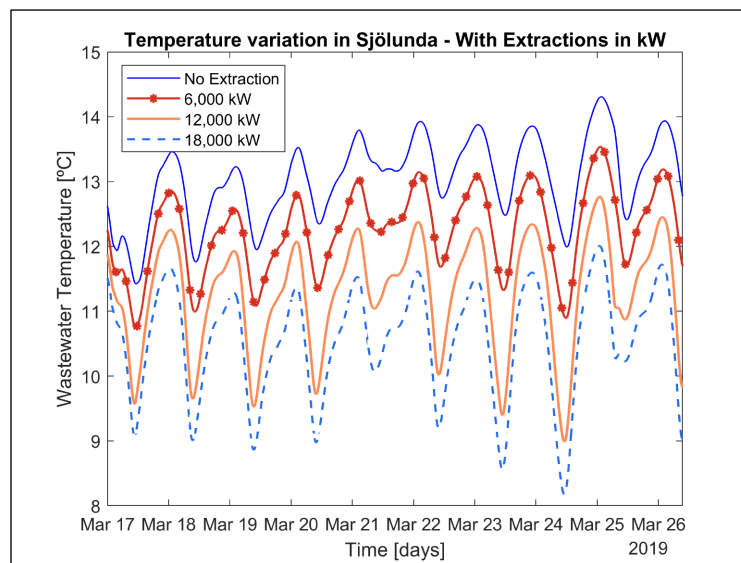


Figure 4.25. Temperature variations at the WWTP for different heat recovery alternatives

2,000 kW, 4,000 kW, and 6,000 kW heat energy recovery is simulated at each pumping station leading to 6,000 kW, 12,000 kW and 18,000 kW heat recovery in total, respectively. The most noticeable effects (downstream) of heat extraction are the lower peaks obtained when the flow rate is reduced due to the daily changes in flow from the households. For example, for smaller flows, a bigger decrease in wastewater temperature at the site of extraction occurs, and for bigger flows, that reduction is smaller. This is because the available energy is a function of both temperature and flow rate. For a better understanding of these singularities, Figure 4.26. and Figure 4.27. show a comparison between a linear reduction of 3 °C from the original downstream temperature (mimicking just vertical movement of the plot), and the result from the modeling process after extracting 36,000 kW (that would give a decrease of around 3 to 6.2 °C). In the latter, the temperature drops are easily noticeable, and they are linked with the reduction of flow from the households during the night.

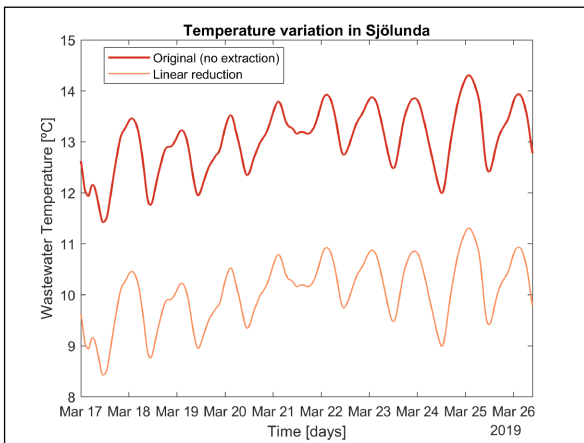


Figure 4.26. Linear temperature reduction at the downstream end.

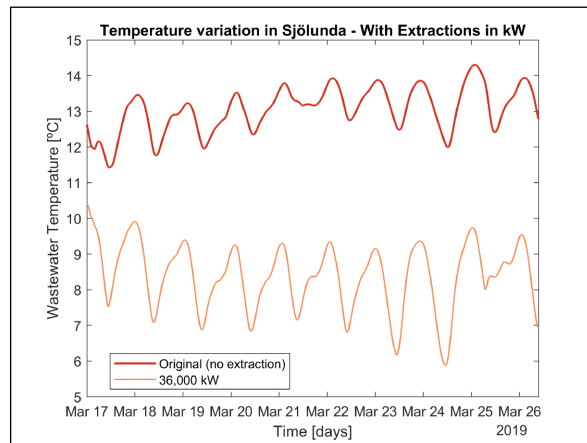


Figure 4.27. Temperature reduction with a recovery of 36,000 kW.

For this reason, another modeling process was conducted, this time simulating a 12-hour heat extraction of 36,000 kW (12,000 kW at each pumping station) during the day, when the temperatures and flows are higher, between 10:00 AM and 10:00 PM. The result can be seen in Figure 4.28., where even after an extraction of that value, the estimated temperature at the WWTP was always over 9 °C, comparable to a 24-hour extraction where a minimum of 5.8 °C was reached. In this case, when cooler peaks occurred with the 24-hour extraction, higher peaks were present in the 12-hour extraction this time in the warmer direction. This means that the 12-hour scheme allows for a positive effect that allows for warm peaks where previously they were tending to go down to the colder temperatures in the 24-hour extraction model.

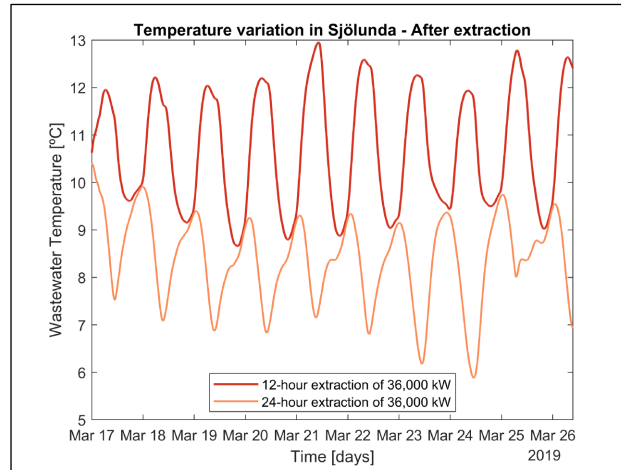


Figure 4.28. Scheme of only diurnal extractions of 36,000 kW (12,000 kW at each PS)

Similarly, an analysis of the energy recovered was done, where the modeled heat recovery value of 36,000 kW, calculated under ideal heat transfer without any losses, corresponds to approximately 316 GWh/year. That value is almost 5% of the total energy consumption of Malmö, that has been around 7 TWh/year for the last 15 years. Also, that value corresponds to 13% of the district heating system in the city, which is in average 2.5 TWh/year. Additionally, the previously values of 6,000 kW, 12,000 kW, and 18,000 kW, correspond to 2.1%, 4.2%, and 6.3% of the total district heating energy consumption of Malmö assuming a 24-hour recovery period.

### S2. Modeling heat recovery from the 1.6 km stretch using the two-week collected data

The results from extracting heat using the data from the two-week period in the 1.6-km stretch in Malmö allowed for an additional substantiation related to how the wastewater flow volume affects the extraction of heat. Here, the amount of heat to be recovered was small compared to that estimated at the pumping stations. The reason behind this is that the flow in this stretch is just a tiny percentage of the flow through the pumping stations. Figure 4.29. shows the resultant wastewater temperature downstream after recovering 500 kW at the upstream end, along with the measured temperature data for the same period. In the figure, when flows decrease, the drop of the temperature increases significantly. To link this result, Figure 4.30. shows the flows at this stretch during the same period. In that figure, the low peaks in flow correspond to those in temperature when heat recovery is done when the flows decrease.

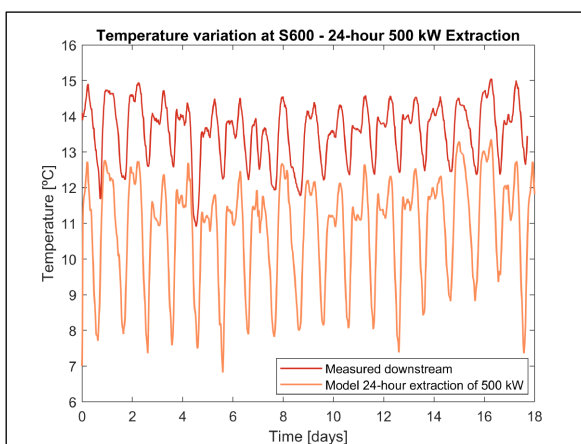


Figure 4.29. Temperature reduction at the well S600 with a recovery of 500 kW.

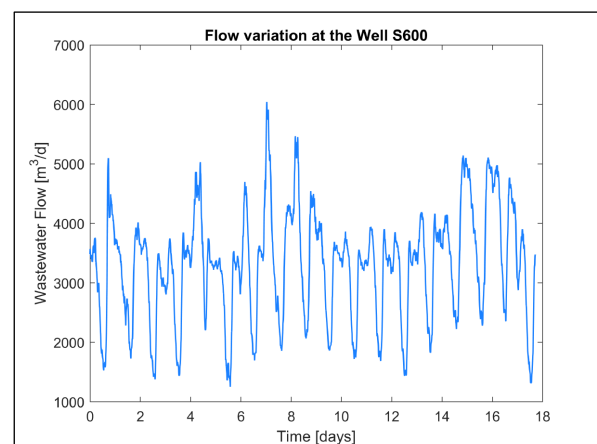


Figure 4.30. Flow variation at the 1.6 km stretch during the two-week period.

Comparably, an additional recovery strategy was implemented where the heat was extracted at the same place but only during the day, a time when the flows and temperatures are higher. This strategy contemplated recovery between 10:00 AM and 10:00 PM. The result of this is shown in Figure 4.31. There it can be observed that the wastewater temperature drop during the extraction times, but when there is no extraction the temperature does not change. Also, this alternative works better than recovering heat during a 24-hour period because the lowest temperature in the former case remains above 10 °C, where the value in the 24-hour case was around 7 °C. Additionally, the recovery model shows that even with a recovery of 500 kW, almost the same temperature ranges are maintained in the wastewater like when no recovery is happening. This can be seen in Figure 4.31. by comparing the result with the measured values measured at the downstream well. Thus, suggesting that heat recovery may be implemented at certain times without affecting the temperatures of the wastewater. Finally, a similar analysis like in the pumping stations case, the value of 500 kW under a 12-hour and 24-hour extraction would supply with energy for a year to 87 and 175 people respectively (considering the average energy consumption per person un Malmö, which is 25 MWh/year per person).

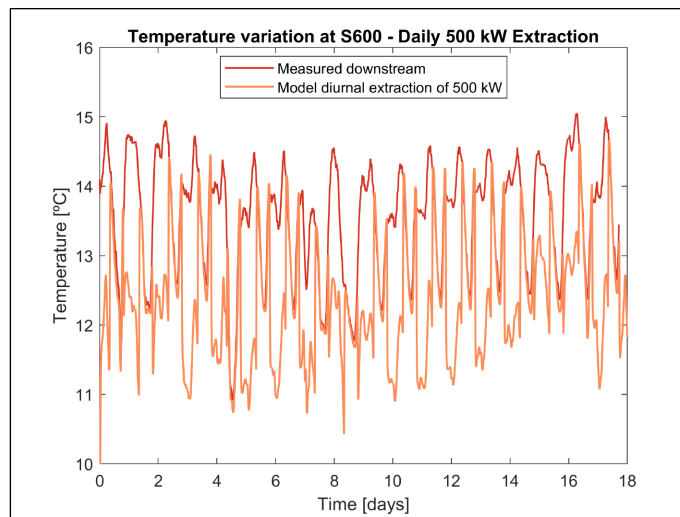


Figure 4.31. Scheme of only diurnal extractions of 500 kW at each the 1.6 km stretch

### ***S3. Modeling heat recovery from the PSs to the wastewater treatment plant using the calibrated flows model and average wastewater temperatures***

When modeling the heat recovery of 18,000 kW in a scenario where the flows for the simulation were the result of using the previously calibrated flow model and similar temperature changes to those gathered in the measurements in the city, an estimated temperature at the WWTP was obtained. Assuming a dry weather condition, the result of modeling with these two inputs during a two-week period delivered an average temperature for the WWTP of around 10 °C. The flows obtained from the BSM-UWS model are shown in Figure 4.32., where the daily patterns are clear, and their values are similar to the average values measured at the pumping stations during 2017 and 2018. Similarly, the input temperatures for this scenario (S3) are shown in Figure 4.33. Those temperatures were obtained from creating average hourly values from the measurements taken during the two-week data collection campaigns.

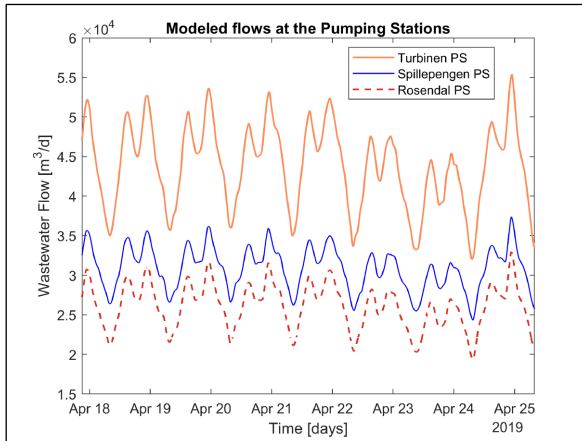


Figure 4.32. Modeled flows for the scenario at the PSs

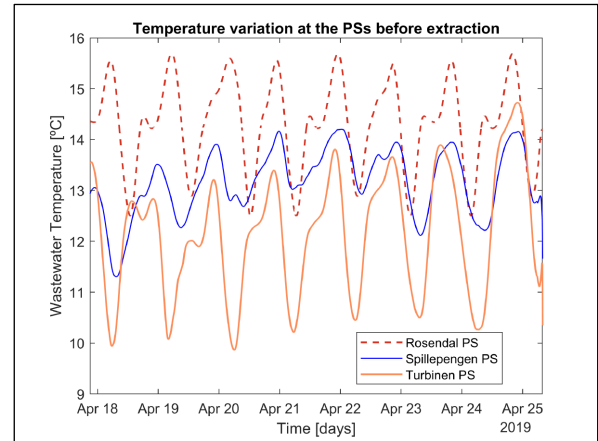


Figure 4.33. Temperature variation profiles created for the scenario at the PSs.

The result from modeling the recovery of 18,000 kW in the proposed scenario is shown in Figure 4.34. In that figure, the fluctuation between the lower and the higher temperatures is between 9 and 11 °C. If this is assumed to be a general scenario for Sjölanda, it can be said that the temperatures are in a safe range and would not harm the biological processes. However, because the precipitation is not being considered and precipitation has the potential to lower the temperature of the wastewater even more drastically, a lower recovery alternative should be implemented under rainy conditions.

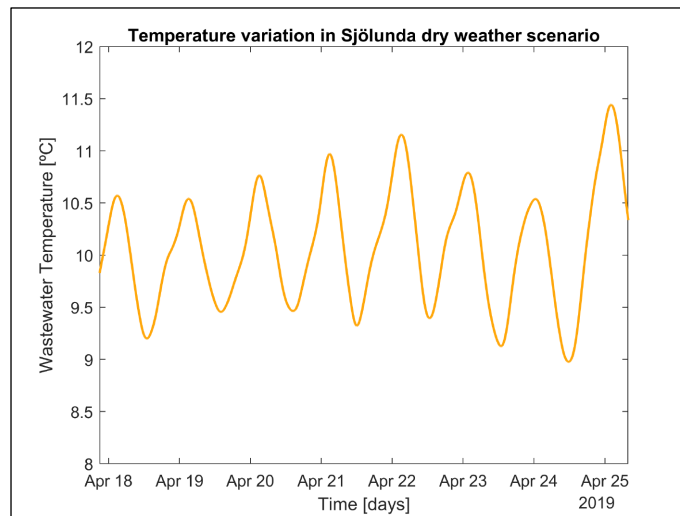


Figure 4.34. Temperature variation at the WWTP in a scenario of an 18,000-kW recovery alternative with modeled flows and estimated temperatures at the upstream end (PSs).

In sum, even though this model was based on estimated flows and assumed temperatures, it gives a baseline of the potential heat recovery that can be obtained and shows how the modeling tools allow for simulating the potential recoverable energy prior to costly infrastructure investments.



## 5 Conclusions

A good calibration of the wastewater flows for the city-wide model for Malmö (using a model in the same environment that the temperature model) was achieved for both dry and wet weather conditions. For wet weather conditions, the difference between the model and the measured values for Turbinen, Rosendal, and Spillepengen, was in average 4,000, 1,000, and 200 m<sup>3</sup>/day respectively, which corresponds to 10%, 4%, and 1% of their average daily flow.

An improvement of the heat transfer model that allowed for a more accurate description of the measured data was achieved. This allowed for the prediction of the temperature variations during day and night in the sewer system in Malmö using easy-to-get parameters within ranges found in literature and using measured flows and temperature data from the upstream and downstream ends of the places under study. The wastewater temperature was predicted with differences between measured and modeled data ranging from 0.1 to 0.3 °C in both day and night periods for the 1.6km stretch, and between 0.1 and 1.2 °C for the stretch between the pumping stations and the wastewater treatment plant.

Three different heat recovery scenarios were analyzed. The first one between the PSs and the WWTP, where 6,000 kW, 12,000 kW, and 18,000 kW heat recovery individual simulations always allowed for a temperature at the WWTP over 8 °C using the two-week period measured data. Also, in the same stretch, a simulated extraction of 36,000 kW (12,000 kW at each pumping station) gave a decrease of around 3 to 6.2 °C from the originally modeled temperature without any extraction. Finally, a modeled heat extraction of the same 36,000 kW, between 10:00 AM and 10:00 PM, resulted in a temperature at the WWTP over 9 °C at all times, comparable to the previous scenario, where during the 36,000kW, 24-hour extraction a minimum of 5.8 °C was reached. A second scenario, a 24-hour extraction of 500 kW at the 1.6 km stretch using the two-week collected data, estimated temperatures down to 7 °C at the downstream end. Similarly, in the same stretch, a 500-kW heat recovery between 10:00 AM and 10:00 PM resulted in a temperature at the downstream end over 10 °C at all times. The third scenario was done using the calibrated flows model and similar temperatures to those gathered from the measurements in the city. In this latter scenario, an extraction of 18,000 kW of heat always kept the temperature at the WWTP over 9 °C. Finally, it was determined that the value corresponding to 36,000 kW is almost 5% of the total energy consumption of Malmö and 13% of the district heating system in the city.

Between the two analyzed alternatives for heat recovery (PSs to WWTP and in the 1.6 km stretch), the most suitable location for heat recovery from the sewer system for the city of Malmö is in the pumping stations because of the high volume flows in those places, which allow for a greater potential of heat recovery without affecting the processes at the WWTP. In these locations, under the measured conditions in the second week of March 2019, an estimated 12,000 kW or 4,000 kW at each pumping station was calculated to be recoverable on a non-stop basis without decreasing the temperature at the WWTP under 9 °C.

A city-wide heat transfer model for the sewer system at a pumping station level was linked with an existing sewer flow model for the same structures in the sewer system to estimate the amount of heat recovery under three assumptions: the flows used were the results from the modeling process using the previously calibrated flow model for dry weather conditions; the temperatures were obtained by similar temperatures obtained in the measurements campaign during the dry

week in March 2019; the limit for heat extraction was set to the estimated downstream temperature (at the WWTP) of around 10 °C. The resulting estimate was a recovery of 18,000 kW, lower than that calculated with the measured data. This probably happened due to the dry weather condition.

The potential of heat recovery from sewer systems was positively determined under different conditions. This opens up the opportunity of implementing sustainable solutions for the reuse of wastewater heat in the sewer systems; solutions that, until this point, have been largely unexploited. The amount of heat that can be recovered from a city like Malmö would reduce the net energy consumption of the water system and decrease the carbon footprint, allowing for a more sustainable way of living that benefits the whole population.



## 6 Future Work

This thesis work explored the temperature changes in the wastewater in the sewer system in Malmö and has answered important questions, such as how much heat can be recovered assuming 100% equipment efficiency. Though, even more questions have arisen from this project. For example, how will the variations in wastewater flow and temperature through the year affect or contribute to heat recovery alternatives. This means understanding if the seasonal changes of temperature will affect the rates of extraction and how that heating and cooling effect of the seasons, paired with the hot water usage from the houses, will affect the final recovery value. Gathering this information will require measurement in other parts of the sewer system, like in stretches within Rosendal and Spillepengen; immediately out of households; and, perhaps most importantly for increasingly accurate modeling, the inlet of the wastewater treatment plant. Similarly, a modeling process using data from households integrated with the calibrated flows model will contribute to the creation of a city-wide flows and temperature model of Malmö. Integration of household wastewater generation, with the calibrated flows model, along with the heat transfer model, will allow for the modeling of different scenarios for population, flows, and temperature changes in the future. Additionally, heat recovery alternatives, including the efficiency of different heat pumps, should be studied to determine the real amount of heat that can be extracted from the system.



## 7 References

- Abdel-Aal, M., Smits, R., Mohamed, M., De Gussem, K., Schellart, A. & Tait, S. (2014). Modelling the viability of heat recovery from combined sewers. *Water Science and Technology*, 70(2), 297-306.
- Abdel-Aal, M., Schellart, A., Kroll, S., Mohamed, M. & Tait, S. (2018). Modelling the potential for multi-location in-sewer heat recovery at a city scale under different seasonal scenarios. *Water Research*, 145(1), 618-630.
- Andrén, S. (2009). Malmö and the urban energy challenge - Some considerations with inspiration from political ecology. Working paper, Human Ecology Division, Lund University.
- Dürrenmatt, D. J. & Wanner, O. (2008). Simulation of the wastewater temperature in sewers with TEMPEST. *Water Science and Technology*, 57(11), 1809-1815.
- Dürrenmatt, D. J. & Wanner, O. (2014). A mathematical model to predict the effect of heat recovery on the wastewater temperature in sewers. *Water Research*, 48(1), 548-558.
- Florides, A. G. & Kalogirou, A. S. (2005). Annual ground temperature measurements at various depths. In: *Clima, 8th REHVA World Congress*. Lausanne, Switzerland, 9-12 October 2005. Cyprus: Higher Technical Institute.
- Frijns, J., Hofman, J. & Nederlof, M. (2013). The potential of (waste)water as energy carrier. *Energy Conversion and Management*, 65(1), 357-363.
- Grmela, J., Kopp, R. & Hadašová, L. (2014). Eutrophication potential of wastewater treatment plants in the upper reaches of svratka river. *Acta Universitatis Agriculturae et Silviculturae Mendelianae Brunensis*, 62(3), 469-475.
- Gustafsson, M., Rayner, D. & Chen, D. (2010). Extreme rainfall events in southern Sweden: Where does the moisture come from?. *Tellus Series A: Dynamic Meteorology and Oceanography*, 62(5), 605-616.
- Haghighatafshar, S., Nordlöf, B., Roldin, M., Gustafsson, L.G., la Cour Jansen, J. & Jönsson, K. (2018). Efficiency of blue-green stormwater retrofits for flood mitigation - Conclusions drawn from a case study in Malmö. Sweden. *Journal of Environmental Management*, 207(1), 60-69.
- Hernebring, C., Milotti, S., Kronborg, S.S., Wolf, T. & Mårtensson, E. (2015). Skyfallet i sydvästra Skåne 2014-08-31: Fokuserat mot konsekvenser och relation till regnstatistik i Malmö. *VATTEN - Journal of Water Management and Research*, 71(2 15), 85-99.
- Malmö stad. (2018). *Malmö - Sweden's fastest-growing city*. [online] Available at: <<https://malmo.se/Kommun--politik/Fakta-och-statistik/In-english/Demographics/Population-growth.html>> [Accessed: 12 February 2019].

- Mikkonen, L., Rämö, J., Keiski, R. L., Pongrácz, E. (2013). Heat recovery from wastewater: Assessing the potential in northern areas. In: Water Research at the University of Oulu, *WaRes Conference*. Oulu, Finland, August 2013. Oulu: Erweko Oy.
- Olsson, G., (2012). *Water and Energy - Threats and Opportunities*. London: IWA Publishing.
- OpenStreetMap contributors, 2019. Aerial view of Malmö - Malmö, Sweden, EPSG: 3008 Projected coordinate system for Sweden, 121339,6160888, [online] Available through: <<http://tile.openstreetmap.org/{z}/{x}/{y}.png>>. [Last Accessed: 15 May 2019]. Data is available under the Open Database License, and if using our map tiles, that the cartography is licensed as CC BY-SA.
- Saagi, R., Flores-Alsina, X., Fu, G., Butler, D., Gernaey, K.V. & Jeppsson, U. (2016). Catchment & sewer network simulation model to benchmark control strategies within urban wastewater systems. *Environmental Modelling and Software*, 78(1), pp. 16-30.
- Saagi, R., Flores-Alsina, X., Kroll, S., Gernaey, K. V. & Jeppsson, U. (2017). A model library for simulation and benchmarking of integrated urban wastewater systems. *Environmental Modelling and Software*, 93(1), 282-295.
- Saagi, R., Arnell, M., Reyes, D., Sehlén, R. & Jeppsson, Ulf. (2019). Modelling heat transfer in the sewer system - towards a city-wide model for heat recovery from wastewater. in: Watermatex 2019. Copenhagen, Denmark. 1 - 4 September 2019.
- Schmid, F. (2008). Sewage Water: Interesting Heat Source for Heat Pumps and Chillers. In: *9th International IEA Heat Pump Conference*. Zürich, Switzerland, 20 - 22 May 2008.
- Sitzenfrei, R., Hillebrand, S. & Rauch, W. (2017). Investigating the interactions of decentralized and centralized wastewater heat recovery systems. *Water Science and Technology*, 75(5), 1243-1250.
- Sörensen, J. & Mobini, S. (2017). Pluvial, urban flood mechanisms and characteristics - Assessment based on insurance claims. *Journal of Hydrology*, 555(1), 51-67.
- Statistics Sweden. (2018). *Population in the country, counties and municipalities on 31/12/2017 and Population Change in 2017*. [online] Available at: <[https://www.scb.se/en/Home/Finding statistics/Population/Population statistics](https://www.scb.se/en/Home/Finding_statistics/Population/Population_statistics)> [Accessed: 12 February 2019].
- UNESCO. (2018). *The united nations world water development report 2018: nature-based solutions for water*. [online] Available at: <<https://unesdoc.unesco.org/ark:/48223/pf0000261424>> [Accessed: 16 May 2019]
- VA Syd. (2017). *Åtgärdsplan för Malmö's Avloppsledningsnät 2017*. [online] Available at: <<https://www.vasyd.se/-/media/Documents/Informationsmaterial/Vatten-och-avlopp/Atgard-splaner-for-avlopp/tgrdsplan-Malm-Avloppsledningsnt-2017.pdf>> [Accessed: 12 February 2019]

Wanner, O., Panagiotidis, V., Clavadetscher, P. & Siegrist, H. (2005). Effect of heat recovery from raw wastewater on nitrification and nitrogen removal in activated sludge plants. *Water Research*. 39(19), 4725-4734.

Water.org. (2019). *Water Crisis Facts - 1 In 9 Lack Safe Water*. [online] Available at: <<https://water.org/our-impact/water-crisis/global-water-and-sanitation-crisis/>> [Accessed: 13 February 2019].



# Table of Abbreviations

*Table 0.1. Table of abbreviations used in this document*


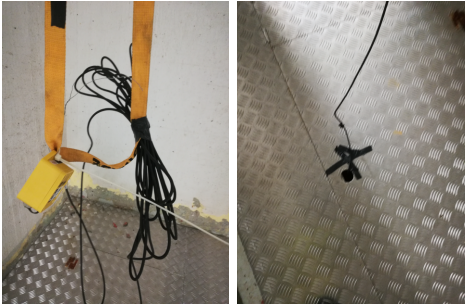


<b>Abbreviation</b>	<b>Full name</b>	
<b>AM</b>	Ante meridiem or before midday	
<b>BSM-UWS</b>	Catchment and sewer network model within urban wastewater systems	
<b>COD</b>	Chemical oxygen demand	
<b>COP</b>	Coefficient of performance	
<b>FAO</b>	Food and Agriculture Organization of the United Nations	
<b>GIS</b>	Geographic information system	
<b>IEA</b>	Department of Industrial Electrical Engineering and Automation at Lund University	
<b>OS</b>	Operative system	
<b>OSM</b>	OpenStreetMap	
<b>PE</b>	Population equivalents	
<b>PM</b>	Post meridiem or past midday	
<b>PS</b>	Pumping station	
<b>PSs</b>	Pumping stations	
<b>RISE</b>	Research Institutes of Sweden	
<b>SMHI</b>	Swedish Meteorological and Hydrological Institute	
<b>SNB</b>	Manhole on the wastewater pipeline	
<b>WWTP</b>	Wastewater treatment plant	
<b>Symbol</b>	<b>Unit of</b>	<b>Name</b>
<b>°C</b>	Temperature	degree Celsius
<b>K</b>	Temperature	kelvin
<b>m</b>	Length	meter
<b>W</b>	Power	watt
<b>kg</b>	Mass	kilogram
<b>J</b>	Energy	Joule
<b>ha</b>	Area	hectare





# Appendices

Table 0.1. Log table created for the first visit corresponding to the installation day of the temperature sensors. (**Tt**: Tinytag number, **ST**: Start time, **CP**: Coordinate point).

Time	Place	Action/Comment	Photos
8/3/2019 9:40 am	Rosendal PS	<b>Tt</b> 860052; <b>ST</b> 10:10 am; Inside the inflow basin in medium velocity flow (not completely still), approximately 25 to 30 cm into the water from the water surface; this was the first installed sensor that day. Also, metal weights were installed to give it a vertical direction and avoid extreme movements. <b>CP</b> 55°36'33.7"N 13°01'39.2"E	
8/3/2019 10:34 am	Spillepengen PS	<b>Tt</b> 860068; <b>ST</b> 10:45 am; Installed right by the inflow channel to the PS, with a high-velocity flow, and near the surface due to the risk of changes in the water level and an increased risk of debris getting attached to the sensor and the weight. <b>CP</b> 55°37'24.2"N 13°03'20.7"E	
8/3/2019 12:00 pm	Strandshems PS	<b>Tt</b> 860056; <b>ST</b> 12:15 pm; Installed in a PS that has a variable water level, however, the sensor was installed where all the time would have water around it and the risk of debris forming around is low because there is only vertical movement of water. <b>CP</b> 55°37'34.4"N 13°02'13.4"E	
8/3/2019 2:06 pm	Turbinen PS	<b>Tt</b> 860087; <b>ST</b> 2:15 pm; Sensor installed in what the team assumed to be the inflow of pure wastewater according to plans of the site. This need to be verified. <b>CP</b> 55°36'16.9"N 12°58'52.8"E	











Time	Place	Action/Comment	Photos
8/3/2019 2:57 pm	well SNB 2417 water	Tt 860081; ST 3:10 pm; Installed in an intersection of two flows with very high and turbulent flow. Additional weights were installed to give more stability to the sensor, also some protection against rats was given to the cable connected to the logger. CP 55°35'03.8"N 12°57'19.4"E	
8/3/2019 3:32 pm	well SNB 2417 air	Tt 860069; ST 3:45 pm; installed to measure the air temperature about 15 to 20 cm over the water level. CP 55°35'03.8"N 12°57'19.4"E	
8/3/2019 4:10 pm	well SNB 2427	Tt 860063; ST 4:25 pm; The original place was changed due to traffic conditions. The installation was done using VA Syd equipment and the cable was also protected, this time with a white tube. CP 55°34'48.3"N 12°57'21.0"E	

Table 0.2. log table created for the second visit corresponding to the collection data day. (Tt: Tinytag number, ST: Start time, CP: Coordinate point).

Time	Place	Action/Comment	Photos
19/3/2019 9:10 am	Turbinen PS	Tt 860087; There was a big ball of paper all around the weight but thankfully the sensor was clean. However, the water level was approximately 10 cm under the sensor so there was not water temperature recording when visited and it's unknown if that has been happening before. additionally, the sensor was moved to a quieter place in terms of flow. In terms of data, the temperature recordings were very noisy and will be analyzed soon to determine what happened. CP 55°36'16.9"N 12°58'52.8"E	

Time	Place	Action/Comment	Photos
19/3/2019 9:45 am	Rosendal PS	<p>Tt 860052; The sensor was found almost clean (just a layer of paper around) and in a very calm flow. The data displayed showed a cleaner and more constant graph which for now seems like a very good result. CP 55°36'33.7"N 13°01'39.2"E</p>	
19/3/2019 10:22 am	Well SNB 2417 water	<p>Tt 860081; The tip of the sensor appeared to be completely clean and the installed protection seemed to work. Also, the data was represented by a mostly smooth and noiseless graph. CP 55°35'03.8"N 12°57'19.4"E</p>	
19/3/2019 10:22 am	well SNB 2417 air	<p>Tt 860069; The sensor had some dirt covering it so maybe it had been covered by wastewater but that will be check later when analyzing the results. CP 55°35'03.8"N 12°57'19.4"E</p>	
19/3/2019 10:28 am	well SNB 2427	<p>Tt 860063; Sensor was clean, the data smooth and the only dirty part was the weight. CP 55°34'48.3"N 12°57'21.0"E</p>	
19/3/2019 10:36 am	Spillepengen PS	<p>Tt 860068; Surprisingly, this sensor was almost clean, and the graph also showed a smooth profile. However, the analysis of the collected data needs to be done. CP 55°37'24.2"N 13°03'20.7"E</p>	

Time	Place	Action/Comment	Photos
19/3/2019 11:12 am	Strandshems PS	Tt 860056; The sensor was mostly clean here and the data showed a smooth profile without so much noise. The real name of this PS is Strandshems. CP 55°37'34.4"N 13°02'13.4"E	

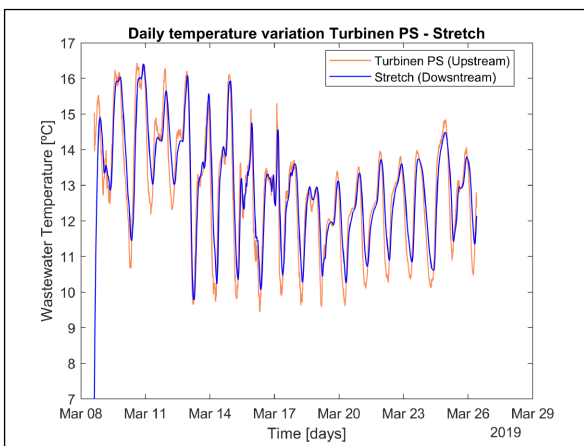


Figure 0.1. Temperature variation in the stretch between Turbinen PS and the point before mixing with the flows from Rosendal PS.

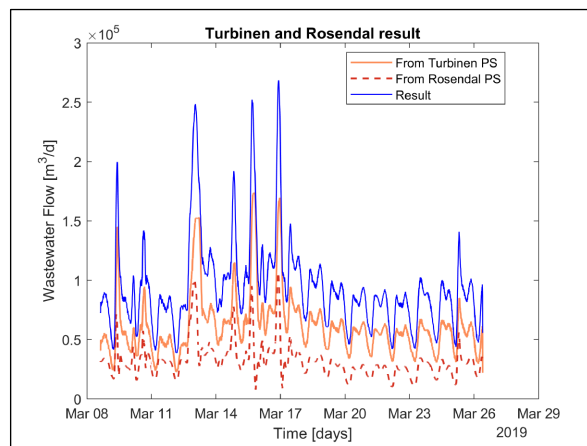


Figure 0.3. Resulting flow from mixing the wastewater flow from Turbinen and Rosendal

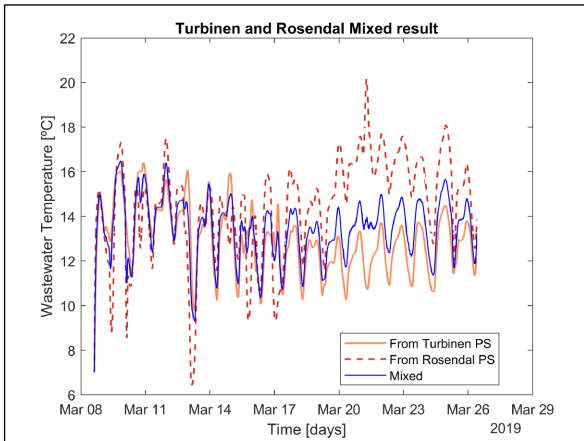


Figure 0.2. Resulting temperature from mixing the wastewater flow from Turbinen and Rosendal

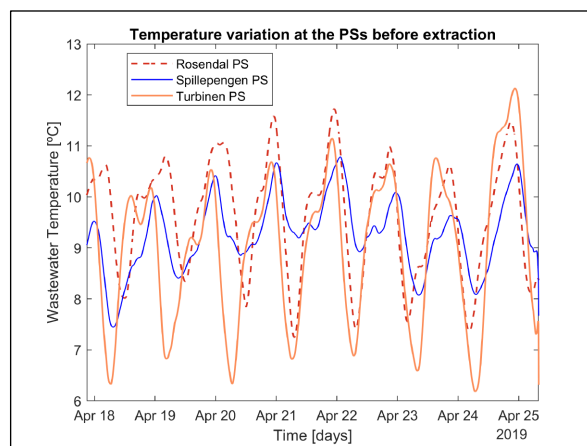
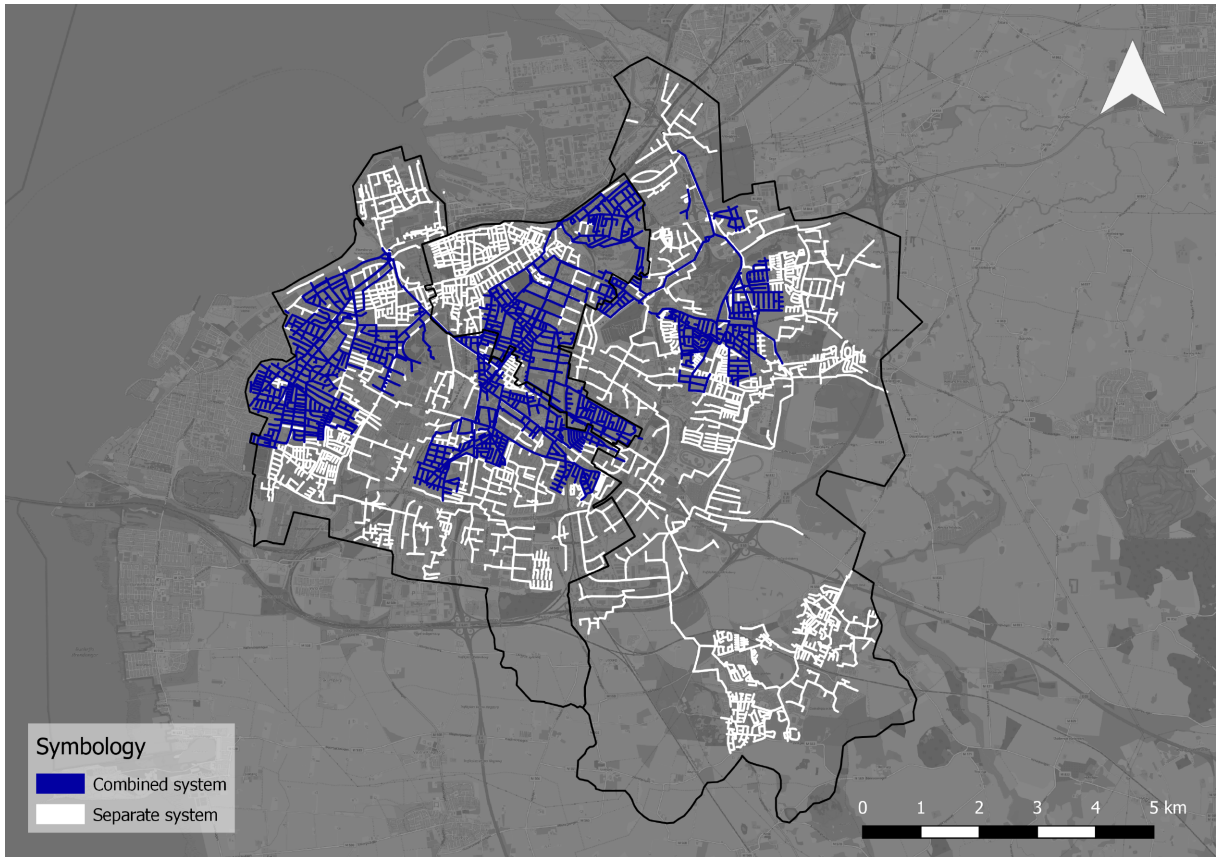


Figure 0.4. Temperature at the pumping stations (upstream end) after an 18,000-kW extraction in the last scenario (S3)



*Figure 0.5. Corresponds to Figure 3.4 "Types of sewer systems in the pipe network in the city." for protanomaly, deuteranomaly, or tritanomaly conditions.*

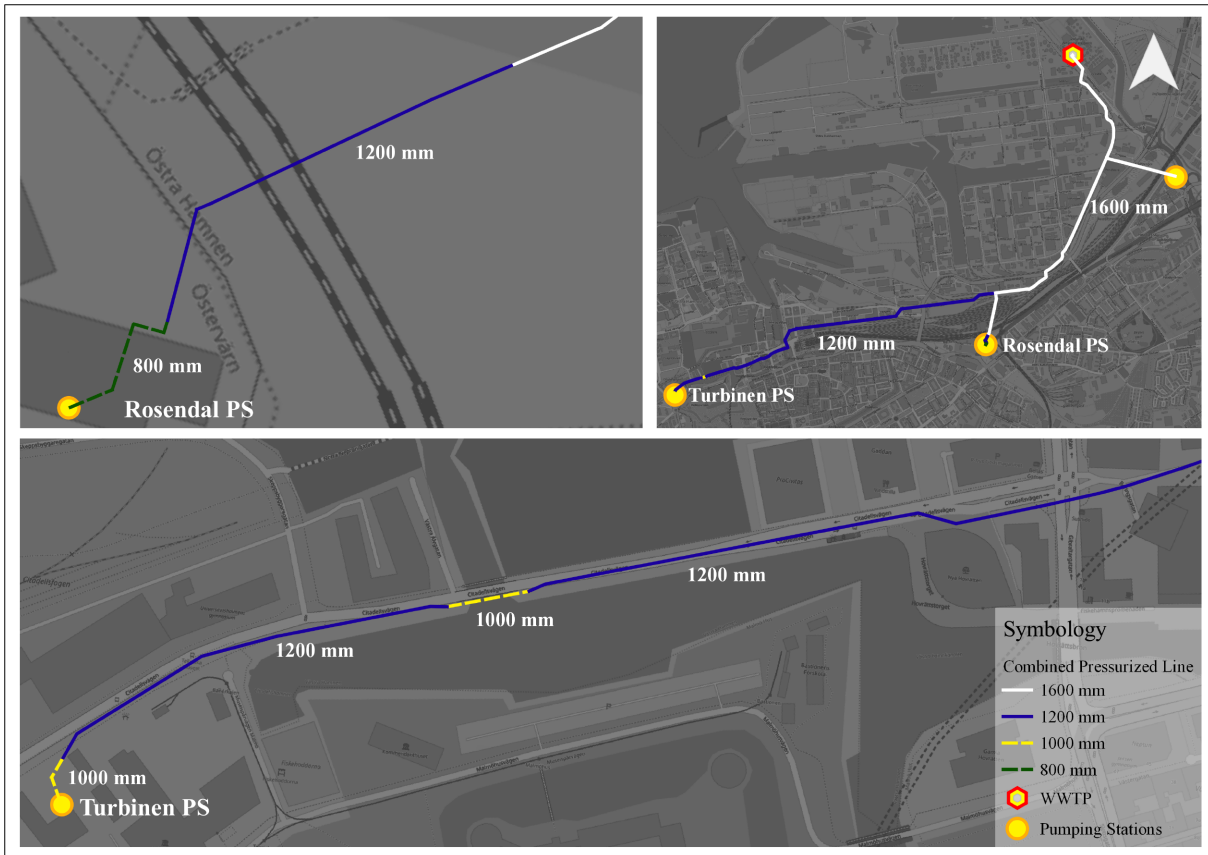


Figure 0.6. Corresponds to Figure 3.10 "Location, scale, and diameters of the pipelines connecting the PSs and the WWTP" for protanomaly, deuteranomaly, and tritanomaly conditions (background map from © OpenStreetMap contributors).

# Popular science summary

## Modeling heat recovery from wastewater systems in Malmö

What if the heat contained in the water released through your sink every morning after showering or brushing your teeth could be transformed in energy for your smartphone? Even more, does reclaiming that heat back to the water so your utility bills would get cheaper sound attractive for you? Well, this project aims to determine how much of that heat can be recovered without affecting the wastewater treatment plant in the city of Malmö using computerized models. Thus, two main steps are followed: modeling the wastewater flow and temperature for the total population of Malmö, and modeling different amounts of heat recovered using field data. The modeling process of the wastewater flows delivered differences as small as 1% between the real and the modeled data. For the temperature model, that difference was between 0.1 and 0.3 °C. Finally, the results from simulation heat extractions from the wastewater suggested that 6.3% of the total energy demand of the district heating in Malmö can be reclaimed maintaining a temperature at the wastewater treatment plant over 9 °C.

Modeling on a city like Malmö can facilitate the decision-making process and lower costs of heat-recovery projects overall due to the estimation of amounts of heat that can be reclaimed. Also, by emphasizing the importance of finding ways to be sustainable, this project aims to deliver solutions to create sustainable cities. For example, tap water heating and the supply for house heating consumes up to 90% of the total energy used in the urban water cycle. Thus, by implementing solutions that allow for the reclaim of that huge amount of energy will reduce the overall energy demand of a city like Malmö.

The work done during the project included the installation of temperature sensors for the wastewater in different places in the city and subsequent visits to those places to collect the registered data. The work also involved office labor and several hours of modeling processes. Finally, is important to say that the results from this project make part of the knowledge that is being created around the amazing topic of heat recovery.